CR-152188

SD 78-AP-0124

DEVELOPMENT OF A CRYOGENIC ROTATING HEAT PIPE JOINT FINAL REPORT

SEPTEMBER 1978

Contract NAS2-9726

(NASA-CR-152188) DEVELOPMENT OF A CRYOGENIC ROTATING HEAT PIPE JOINT Final Report, Nov. 1977 - Sep. 1978 (Rockwell International Corp., Downey, Calif.) 72 p HC A04/MF A01 CSCL 20D G3/34

N78-33384

Unclas 35920

PREPARED FOR
AMES RESEARCH CENTER
NATIONAL AERONAUTICS AND SPACE ADMINISTRATION
MOFFETT FIELD, CALIFORNIA 94035

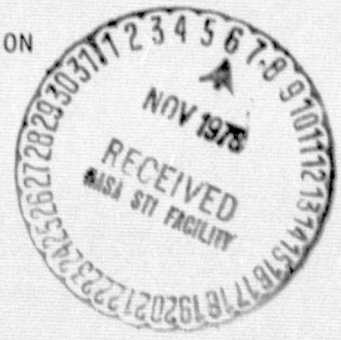

Satellite Systems Division
Space Systems Group

Rockwell International

FOREWORD

This report is submitted by the Space Systems Group of Rockwell International Corporation to the National Aeronautics and Space Administration, Ames Research Center, in accordance with the requirements of Contract NAS2-9726. The work was administered by the Project Technology Branch of the Space Projects Division, with Dr. Craig McCreight as Technical Monitor.

The program was performed under the direction of J. P. Wright, Program Manager. Technical and laboratory assistance was provided by W. S. Robins, C. D. Rosen, and A. L. Striepens. Fabrication of the rotating joint was provided under subcontract by the Rudolph E. Krueger Company of Newport Beach, California.

CONTENTS

CONTENTS (CONTINUED)

LIST OF ILLUSTRATIONS

TABLES

PRECEDING PAGE BLANK NOT FILMED

SUMMARY

The objective of this program was to develop and demonstrate the performance of two critical technology components required for a continuously rotatable heat pipe: (1) a low-leakage rotatable coupling for the heat pipe pressure vessel, and (2) a rotatable internal wick. Performance and leakage requirements were established based on 12 months operation of a cryogenic rotatable heat pipe on a satellite in earth orbit.

ROTATABLE JOINT DEVELOPMENT

A rotatable joint test fixture was designed and built to simulate the rotating section of a cryogenic heat pipe pressure vessel. The joint consisted of a 1.27 cm I.D. by 24 cm long tube with a 7.3 cm diameter housing in the center which contained the dynamic seal components and the static close-out seal. All major components of the housing were made from 17-4 PH stainless steel to minimize differential thermal contraction at cryogenic temperature. The 17-4 steel was selected based on machinability, strength, and conduciveness to plating and polishing.

A schematic of the rotatable joint fixture is shown in Section 2.0 (Figure 2-2). Details of the design are shown in the assembly drawing (Figure 2-3).

The rotating shaft is mounted on ball-bearing assemblies at two locations. The shaft has an outside diameter of 1.6 cm, which is hard chrome-plated and polished in the region of the dynamic seal. The dynamic seal is a 1.6 cm diameter ring with a cross-section as shown in Section 2.0 (Figure 2-2). The seal is forced against the rotating shaft and a diaphragm washer by a spring-loaded wedge ring. The wedge ring and seal are beveled at the point of contact so that the spring force is distributed against the two sealing surfaces.

Several candidate seal materials were considered including pure TFE Teflon[1], TFE Teflon with 12-15% carbon graphite, KEL-F[2], Vespel[2], lead, and gold. These

[1]Tradename—G.I. Dupon De Nemours Company
[2]Tradename—3M Company

were evaluated in terms of hardness, ductility, strength, permeability, and coefficient of friction both at ambient and cryogenic temperatures. Kel-F was found to have the best combination of mechanical properties, although none of the materials were good in every respect. Vespel and graphite-impregnated Teflon were selected as alternates, although the limited scope of this effort permitted testing of only one seal material. Other materials were, however, evaluated and tested under independent research and development efforts at Rockwell. Essential results of this additional effort are reported herein along with the results of the test phase of this program.

Performance testing of the rotating joint was conducted under vacuum conditions at ambient and cryogenic temperatures. Leakage rates were measured as a function of internal pressure, both statically and at a rotational rate of 4 rev/hr. Leakage measurements were made prior to and after a 10,000-cycle wear-in. Prior to wear-in, the static helium leakage rate at ambient temperature and 0.4 Mpa pressure was 1.5×10^{-3} sccs. After wear-in, the leakage rate increased significantly to 1.7×10^{-2} sccs. Inspection revealed that the Kel-F had worn excessively. After repolishing the shaft, testing was repeated on a spare Kel-F seal. This time, the wear-in was limited to 42 cycles at 4 rev/hr. Both static and dynamic leakage rates were lower prior to wear-in and after 20 cycles, but increased by more than an order of magnitude after 42 cycles. Inspection again showed excessive wear on the Kel-F seal.

Independent tests were run on a graphite-impregnated seal, using the same test fixture. Prior to wear-in, the static and dyanamic leakage rate at 0.1 Mpa pressure and ambient temperature was 3.6×10^{-3} sccs. After a 400-cycle wear-in, the static leakage rate reduced to 5×10^{-5} sccs. At cryogenic temperature (115 K), the static and dyanamic leakage rates at 0.4 Mpa were 2.6×10^{-2} sccs and $>1.65\times10^{-2}$ sccs, respectively. The higher values at cryogenic temperatures may be due to increased hardness or elastic modulus of the Teflon/graphite.

The Teflon/graphite seal showed lower torque values compared to the Kel-F (0.1 N-m versus 0.6 N-m).

ROTATABLE WICK DEVELOPMENT

A 0.64 diameter by 12 cm long rotatable wick was designed, fabricated, and functionally tested. The rotating wick assembly, shown in Section 3.0 (Figure 3-7) consists of two sections of tubular screen wick which are joined at the

rotational interface with a two-piece nylon sleeve-type bearing. The wick was a spiral multiwrap composite, consisting of an inner core of 54-mesh screen spirally wrapped over a small mandril and encapsulated by a single layer of 200-mesh screen. The nylon bearing aligns the two wicks and maintains them in proximity such that the interface gap is less than 0.025 cm wide. This controlled-width gap assures that the wick will self-prime in a 1-g field. The nylon bearing provides a smooth low-friction rotational surface; the sleeve bearing clearance is small enough (<0.005 cm) to provide at least the same capillary pumping pressure as the 200-mesh outer screen layer. The nylon bearings are also designed to support the wick concentrically within a heat pipe while allowing space for vapor transport.

Two types of functional tests were performed on the rotating wick assembly. First, a bubble pressure test was performed by submerging the wick slightly in a methanol bath and pressurizing the inside wick volume with gaseous nitrogen. The wick held a pressure of 6.6 cm of water, which corresponds to 96 percent of theoretical for 200-mesh screen. The maximum bubble pressure was not affected by rotation of the wick.

The second test was a self-priming test to determine whether the wick would prime across the rotating interface in a horizontal positon. The test was conducted with the wick assembly on a scale so that the absorbed liquid volume could be measured. Priming of the entire wick was observed, with total priming occurring in approximately two minutes. The absorbed liquid volume agreed with the theoretical fill within 10 percent.

CONCLUSIONS

The essential components of a continuously rotatable heat pipe have been developed, although the leakage rates achieved were higher than the 10^{-6} sccs design goal. The graphite-impregnated TFE Teflon was superior to Kel-F as a seal material in all respects (leakage, torque, and wear-resistance). The rotatable wick joint functioned successfully in terms of capillary pressure, continuity across the interface, and 1-g self-priming.

In conclusion, the feasibility of a cryogenic rotatable heat pipe for long-term space operation hinges on reducing leakage rates to an acceptable level. For some heat pipe working fluids, the leakage values achieved may

well be acceptable for operation up to one year or even longer. Additional testing and development with Teflon/graphite seals is recommended. After acceptable leakage levels have been achieved, fabrication and testing of a rotatable heat pipe based on this rotatable joint and wick technology is also recommended.

1.0 INTRODUCTION

This report summarizes the results of Contract NAS2-9726, *Development of a Cryogenic Rotating Heat Pipe Joint*. The period of performance for the program was from November, 1977, through September, 1978.

BACKGROUND

Flexible cryogenic heat pipes capable of transporting heat across movable interfaces have been developed (Reference 1). Flexible couplings provide efficient heat transfer across hinged joints, such as in a deployable radiator, or across continuously articulating joints such as in a scanning radiometer. There exists, however, a class of applications which require continuous rotation in one direction. Such motion may be required with limb atmospheric scanning radiometers, or with earth or stellar gazing radiometers which must be trained in a particular direction. Other payload subsystems, such as solar arrays or communications antennas, must be pointed in a different direction and maintained there as the spacecraft and orbit precess. To accommodate this type of motion, a heat pipe with a continuously rotatable coupling is required. The rotation in this case is an axial rotation of one end of the heat pipe with respect to the stationary end, and thus requires dynamic slip seal couplings for both the heat pipe container and wick.

REQUIREMENTS

The one-year life translates into a standard helium leak rate requirement of roughly 10^{-3} to 10^{-6} atm-cc/sec (sccs), depending on the heat pipe operating temperature, working fluid, wick design, and allowable excess fluid volume.

The design goal leak rate for the rotatable joint was 10^{-6} sccs of helium at 77 K and at an internal pressure of 0.4 Mpa (58 psia) in a vacuum environment. The maximum rotational torque was 3-5 N-m under operating conditions. While leakage rates of this magnitude are achievable with state-of-the-art rotating seals at ambient temperature, the concurrent requirements for cryogenic temperature operation and high internal pressure render this development a rather aggressive effort with respect to the state of the art. Requirements for the wick, on the other hand, were felt to be less severe and, consequently, the bulk of the effort was devoted to development of the rotatable joint.

2.0 ROTATING JOINT DEVELOPMENT PROGRAM

The purpose of the rotating joint development program was to develop a rotary joint test fixture which would simulate the rotating portion of a rotary heat pipe excluding the wick. Requirements for the joint were defined at the outset of the program based on a heat pipe operating on an orbiting satellite for at least one year. The most critical part of the fixture is the seal itself. A number of seal design concepts as well as material combinations were analytically evaluated. Because of the limited scope of this program, only a single joint and seal material were tested under this contract. The following sections discuss the requirements, design concepts, materials evaluation, the rotating joint design and fabrication, and the test program and results.

REQUIREMENTS

The primary design requirements for a rotating heat pipe joint include leakage, pressure containment, rotational speed and torque, operational life, and materials compatibility between the seal, the container, the working fluid and the wick. The joint was not designed for any specific working fluid or temperature, but rather for any fluid in the range of 77 K to 300 K. Typical heat pipe working fluids in that range include nitrogen, oxygen, methane, ethane, ammonia, and water. A summary of the design requirements specified for this development program are summarized in Table 2-1.

The essential requirement for the joint, of course, is leakage. Since heat pipe performance is generally very sensitive to fluid charge, the allowable leakage must be sufficiently small such that at the end of the operational life, there is still enough fluid to completely saturate the wick with liquid and the remainder of the internal volume with vapor. This requires that there initially be some excess fluid in the heat pipe. If the excess fluid occupies a relatively large volume, a separate excess fluid reservoir would be required to prevent the excess fluid from blocking off the condenser of the heat pipe. For cryogenic heat pipes, a large amount of excess fluid will also significantly

increase the internal pressure at ambient temperature. For these reasons, it would be desirable to keep the excess fluid required to a minimum, which means a low leak rate.

Table 2-1. Rotating Joint Performance Requirements

Parameter	Value
Leakage (design goal)	1×10^{-6} sccs helium
Operating temperature	77 K to 300 K
Operating pressure	0.4 MPa at 77 K
Non-operating pressure	10.1 MPa at 293 K
Proof pressure	20.28 MPa
Burst pressure (min.)	40.55 MPa
Torque	3-5 N-m at 77 K
Rotational speed	4 rev/hr maximum
Life (design goal)	1 year

Assuming laminar flow through the leakage path, for a given leakage of liquid in one year, the required leak rate in terms of helium under standard conditions is given by

$$Q = 3.171\times10^{-8}\ \frac{L}{P_v}\left(\frac{\mu v}{\mu_{He}}\right)\left(\frac{\rho_\ell}{\rho_v}\right)$$

where

L is the liquid loss per year (cm of liquid/year)

Q is the helium leak rate in atm-cc/sec (sccs)

μ_v is the vapor viscosity at operating temperature

μ_{He} is the viscosity of helium under standard conditions

$\left(\frac{\rho_\ell}{\rho_v}\right)$ is the ratio of the vapor-to-liquid density at operating temperature

P_v is the vapor pressure (atm) at operating temperature

Assuming an allowable leakage of 1 cm^3 of liquid in one year under operating conditions, the required helium leak rate for various working fluids at typical operating temperatures is shown in Table 2-2.

The design goal leakage rate of 1×10^{-6} sccs is below all of the required rates shown in Table 2-1 except for nitrogen (0.9×10^{-6} sccs). At ambient temperature, however, the leakage rates for all of the fluids shown in Table 2-2 (except water) will be greater according to the internal pressure

Table 2-2. Helium Leakage Requirements for Various Fluids

Fluid	Temperature (K)	Required Helium Leak Rate (sccs)
Water	300	1.9×10^{-2}
Ammonia	250	3.8×10^{-6}
Ethane	170	3.2×10^{-4}
Methane	110	7.3×10^{-5}
Oxygen	90	2.8×10^{-6}
Nitrogen	80	0.9×10^{-6}

for each fluid. For cryogenic fluids, such as oxygen or nitrogen, the internal pressure at ambient temperature may be up to 100 times greater than at operating conditions. Storage at cryogenic temperature prior to assembly onto a satellite would minimize the loss of fluid, but the pipe may still be exposed to ambient temperature for several weeks or months prior to launch. One possible solution would be to charge the heat pipe *in situ* on the experiment or satellite just prior to launch. Although not specifically addressed in this program, the issue of long-term ambient temperature storage for cryogenic heat pipes will ultimately have to be evaluated.

DESIGN CONCEPTS

Literature and industry surveys were made to evaluate the various types of space and industrial dynamic seal concepts for this application. While a number of dynamic rotating seal concepts for industrial applications were found, none were found that could meet all requirements for high pressure containment, cryogenic temperature operation, and low leakage with helium gas. Conventional O-ring type seals become hard and brittle at cryogen temperature. A fluid swivel joint was developed by Vought Corporation for advanced Shuttle applications using Teflon O-rings (Figure 2-1). While relatively low leakage levels were achieved with Freon liquid, down to 145 K, it is doubtful that this concept could contain a high pressure gas, particularly helium, with acceptable leakage rates. With a liquid, leakage is reduced considerably compared to a gas due to capillary surface tension of the liquid in the region of the leakage path.

Another concept would be to use standard O-rings for the seal, and to build in a large thermal resistance between the seal and the internal tube wall such that the seal would remain at near ambient temperature. This concept

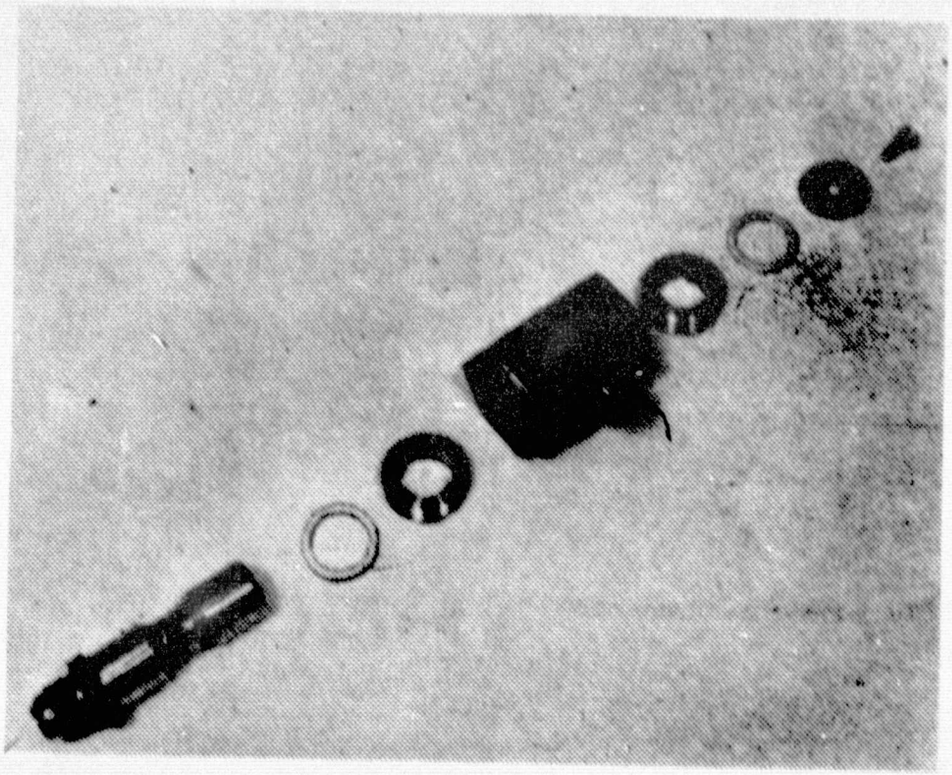

ORIGINAL PAGE IS
OF POOR QUALITY

Figure 2-1. LTV Fluid Swivel Joint

was developed for a liquid helium flow circuit. Although leakage rates were on the order of 1×10^{-6} sccs, the long thin-wall bayonet-type tubing required to minimize the heat leak to the joint would not be suitable for high internal pressure containment requirements.

Another concept which proved to be unsuitable for this application is a ferromagnetic seal. While ideally suited for vacuum-type seals at ambient temperature, ferromagnetic seals cannot be used with high internal pressures or at cryogenic temperature due to the properties of the ferro fluid.

The selected concept involves the use of a soft ring-type seal which is forced against two highly polished sealing surfaces by an internal or external mechanical spring. This allows the shaft and seal housing to be designed for high pressure containment with little distortion of the sealing surface due to either pressure or differential thermal contraction. The use of a metallic spring overcomes the problem of loss of resilience of the seal material at cryogenic temperature. The actual seal design selected for development was based on a design which was developed for the Saturn II J2-S engine oxidizer lines (Reference 2). Details of the rotary joint and seal design are described below.

ROTABLE JOINT DESIGN

To adequately evaluate the cryogenic rotating heat pipe coupling concept, a rotary joint test fixture was designed based on a 1.27-cm (0.5-in.) I.D. heat pipe, and the requirements in Table 2-1. A schematic of the rotary joint test fixture is shown in Figure 2-2. Details of the joint are shown in the assembly drawing, Figure 2-3. The test fixture was designed to permit parametric testing of several seal materials under various conditions of temperature, pressure, rotational rate, and spring loading of the seal.

Rotary Joint Description

The overall envelope of the test fixture is 7.30 cm (2.975 in.) diameter by 24.13 cm (9.50 in.) long and is basically determined by the heat pipe I.D., the support bearing spacing, and the working pressure. Minimizing heat transfer to the joint from the environment during cryogenic testing was also considered. As shown in Figure 2-2, the test fixture comprises two main sections

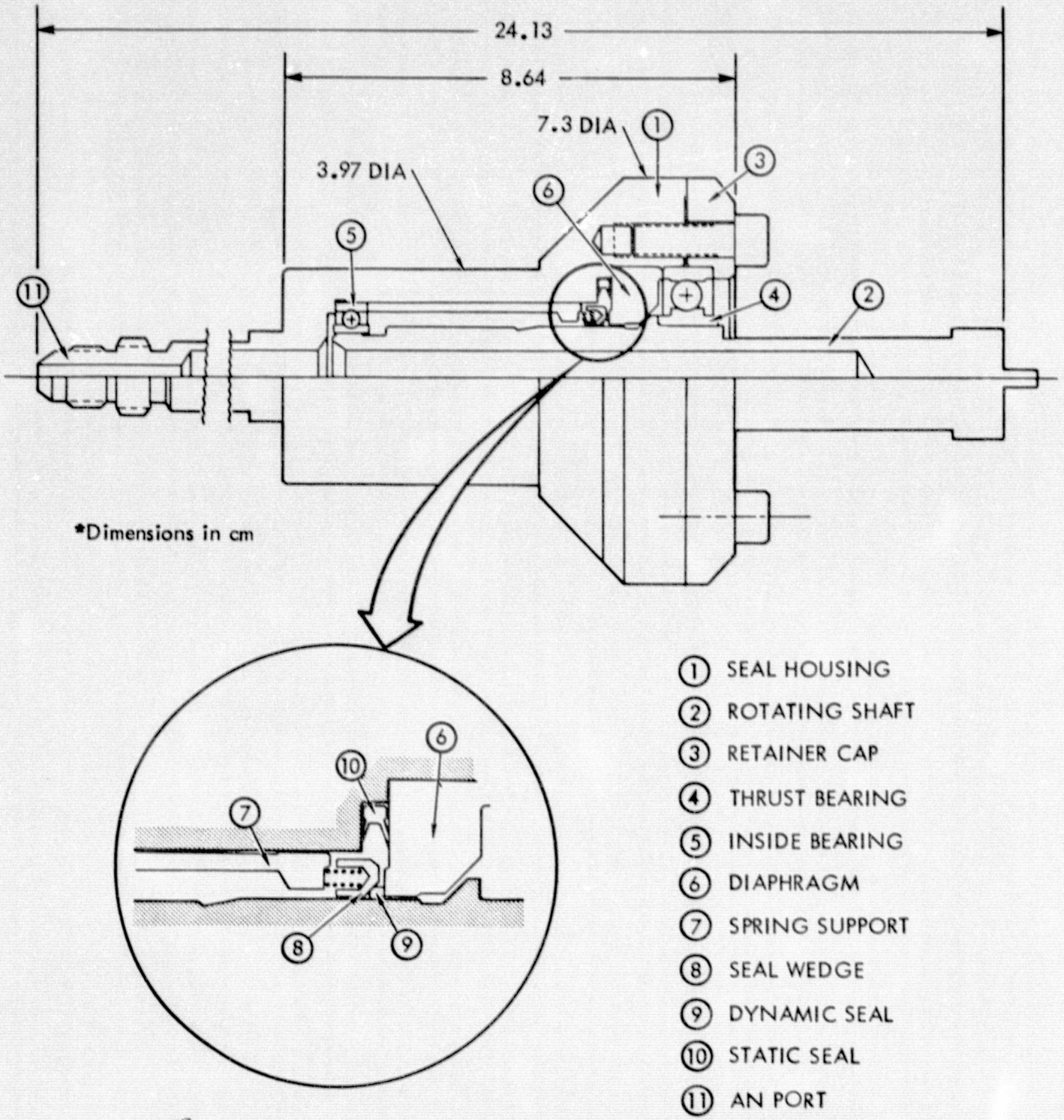

Figure 2-2. Rotating Dynamic Seal Concept

FOLDOUT FRAME 1

ORIGINAL PAGE IS
OF POOR QUALITY

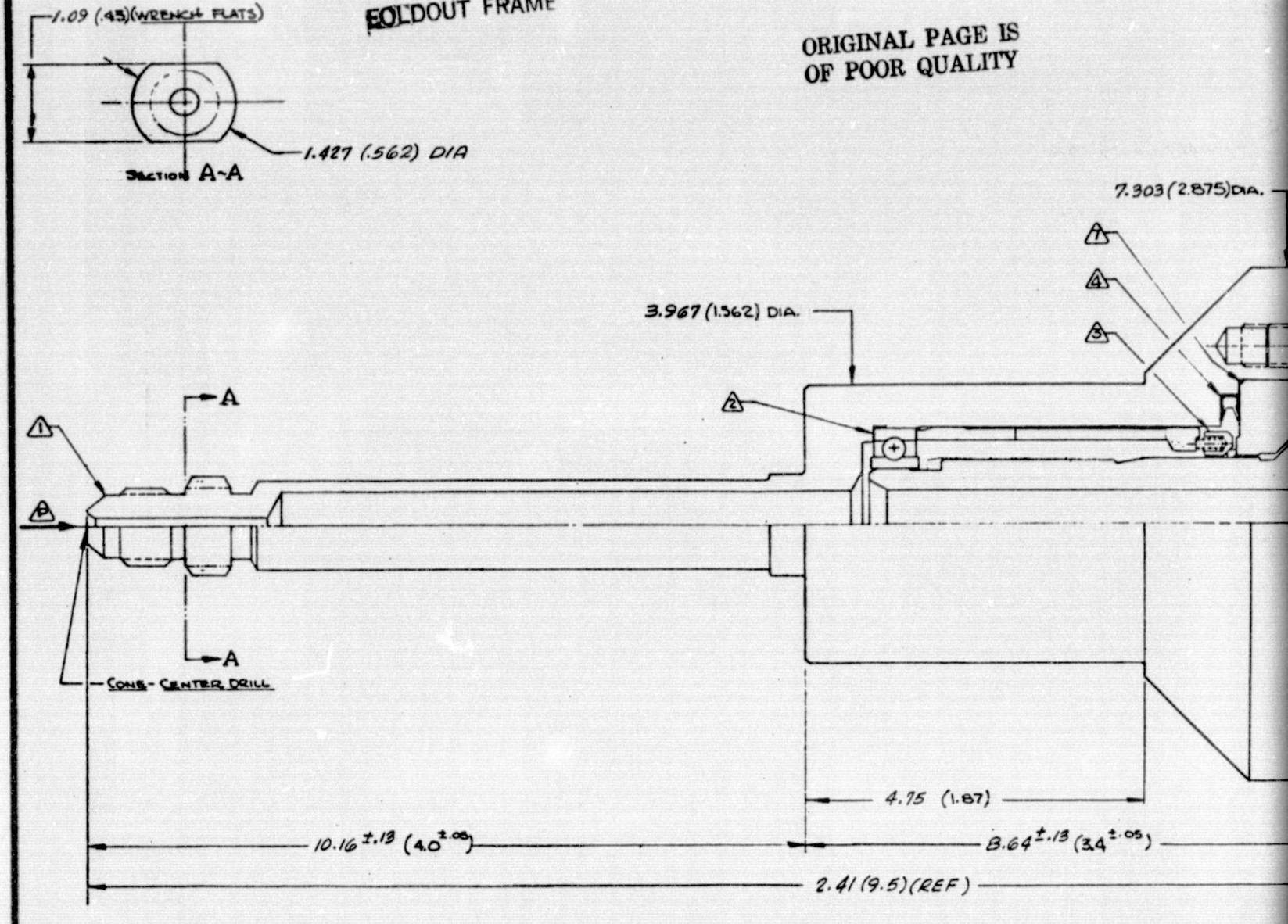

NOTES

1. FITTING END PER AND 10056 FOR .635CM(¼ IN) O.D. TUBE (EXCEPT AS NOTED)
2. FAFNIR B538 BRG.
3. P/N 124385 TG 750 DYNAMIC SEAL (KRUEGER CO.)
4. P/N 12195 CR 1437 STATIC SEAL (HARRISON MFG.)
5. FAFNIR KP12A BRG. (REMOVE GREASE SEALS) (1735 N (3900 LB) THRUST)
6. ¼-28 SOC. HD. CAP SCREW – 8 EA. AT 9074N (2040 LB. ULT. TEN. RATING
7. SEAL SUPPORT

MODIFICATION BY: W.S. ROBIN
REF: SKETCH BY: T. CAFFERTY – R

C	REVISED FOR BURST REQ'MT.	7-78
B	REVISED & REDRAWN	7-78
LTR.	CHANGE	DATE

ACT.
CAL.

Figure 2-3 Assembly Drawing - Rotating Heat Pipe Joint

ORIGINAL PAGE IS
OF POOR QUALITY

OPERATING REQUIREMENTS

- (A) AMBIENT PRESS. ~ VACUUM TO 0.1 MPA
- (T) AMBIENT TEMP ~ 77K TO 320K
- (R) ROTATION ~ 3-4 REV/HR
- (P) PRESSURE
  - 1) OPERATING: ROOM TEMP 10.1 MPA (1455 P.S.I.G)
    CRYOGENIC 0.4 MPA (43 P.S.I.G)
  - 2) PROOF: 20.2 MPA (2925 P.S.I.G.)
  - 3) BURST: 40.4 MPA (5860 P.S.I.G)

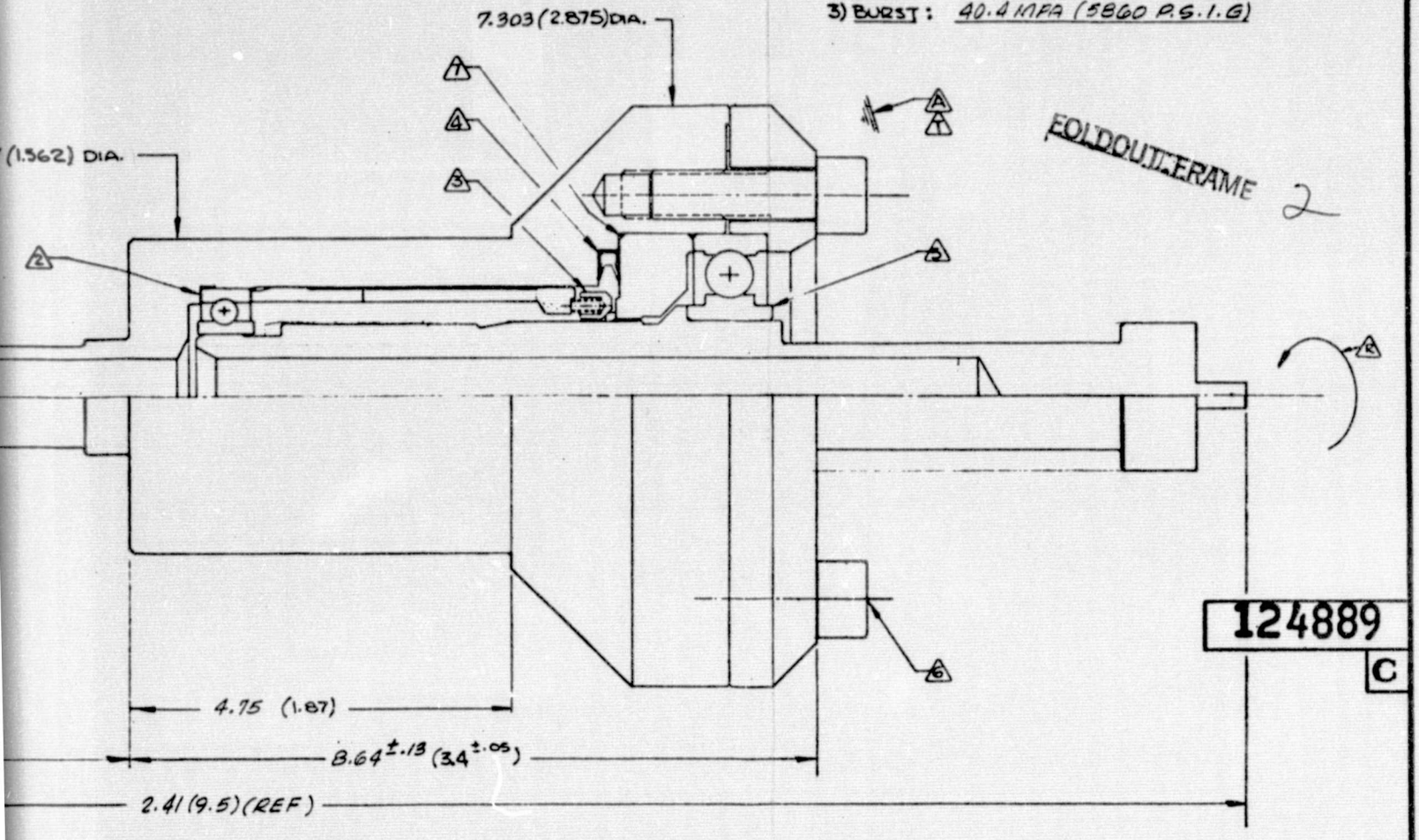

FOLDOUT FRAME 2

124889
C

S NOTED)

UST)
. RATING

MODIFICATION BY: W.S. ROBINS - ROCK. INT'L. 6 JAN. '78
REF: SKETCH BY: T. CAFFERTY - ROCKWELL INTERNATIONAL

C	REVISED FOR "BURST" REQ'MT.	7 JAN '78	R.K.		
B	REVISED & REDRAWN	7 JAN '78	R.K.		
LTR.	CHANGES	DATE	BY	APP.	

NOTICE
THIS DRAWING MAY NOT BE REPRODUCED OR USE THE INFORMATION HEREON USED WITHOUT SPECIFIC PERMISSION

ACT. WT.
CAL. WT.
NO. REQ.
NEXT ASSY.
USED ON

ITEM NO.	QTY. REQ.	SIZE	DESCRIPTION	MILITARY	CODE
		MATERIAL		MATERIAL SPECIFICATION	

UNLESS OTHERWISE SPECIFIED THE FOLLOWING LIMITS APPLY
DECIMAL .XX ± .010, .XXX ± .005
ANGULAR ± 1°
EXTERNAL CORNERS .005 TO .060 R
SURFACE FINISH 125 / MAX.
BREAK SHARP EDGES .005 X 45°
DIMENSIONS TO BE MET BEFORE PLATING

HEAT TREAT
FINISH SPEC.

DRAWN	
APPROVED	
PROJ. ENG.	
OFFICE	
MFG. APPR.	R. KRUEGER 6 JAN '77

DRAWING NO. 16870
SCALE 2 = SIZE
RUDOLPH E. KRUEGER CO.
NEWPORT BEACH, CALIF.

ROTATING JOINT TEST FIXTURE

124889

—a stationary housing (1) with a port (11) through which helium gas is introduced during testing, and a rotating shaft (2) which allows for evaluation of the dynamic seal and rotational torque. The shaft and internal components are secured by a retainer cap (3) which is bolted to the housing (Figure 2-3). The type, number, and spacing of the bolts are determined by the pressure requirement.

Two precision stainless-steel bearings (4) and (5) are used to center and guide the rotating shaft within the stationary housing and are retained by associated support hardware. Leakage from the stationary housing and support hardware is prevented by means of a Teflon-coated metallic static seal (10) which is typical of cryogenic space rated seals. Leakage around the rotating shaft is prevented by a "Delta" seal (9) designed by the R. E. Krueger Company and was selected specifically for this application. This type of seal concept has been successfully used in cryogenic space-rated applications and provides considerable design flexibility in sealing surface configuration and spring loading capability.

To be completely effective, the dynamic seal must prevent leakage from the vertical flat face of the diaphragm (6) as well as around the rotating shaft. This is accomplished through the use of 16 small helical compression springs which force a wedge ring (8) against the plastic seal and at an angle such that a portion of the load is transmitted to the flat face and a portion to the rotating shaft. Should the need arise, the compression spring load, as well as the angle at which the load is applied to the seal, can be altered to change leakage and/or torque.

For test purposes, the rotatable joint has been designed such that a liquid nitrogen chill block can be secured to the outer diameter of the stationary housing to permit testing at temperatures as low as 80-100 K.

Materials and Surface Finish

With the exception of the dynamic shaft seal and bearings, the rotary joint components are fabricated entirely of 17-4 stainless steel to minimize problems associated with thermal contraction during cryogenic testing. This material is also conducive to lapping and/or plating operations which are required on critical sealing surfaces. To provide an adequate sealing surface

for the static seal, the interfaces are machined to a 32 RMS finish as recommended by the seal supplier. For the dynamic seal, the flat vertical seal support face is hard chrome-plated and lapped flat to three helium light bands and the shaft is lapped round, chrome-plated and polished to a waviness within 0.0002 cm/cm.

Leakage at the dynamic seal interface is minimized by insuring that the shaft and its dynamic seal maintain contact during rotation. The concentricity of the bearing support surfaces has been specified to be within 0.008 cm (0.003 in.) TIR.

Pressure Containment

The rotary joint test fixture was designed for an ultimate burst pressure >40.55 MPa (5880 psi) to provide a pressure safety factor greater than 4.0. The joint is made from 17-4 steel (cond. H1150) which has the following properties:

	Ksi	MPa
Ultimate tensile strength	125	862
Tensile yield strength	100	690
Compressive yield strength	90	621
Ultimate shear strength	79	545
Modulus of elasticity	2.85×10^4	1.97×10^5

The calculated burst values and safety factors for the housing and rotating shaft are shown in Table 2-3. The retainer cap was also analyzed for shear of the outer race of the thrust bearing on the inside lip of the cap and for tensile load on the bolts. As shown (Table 2-3), the tensile load on the bolts was the limiting case, with a safety factor of 5.4.

Table 2-3. Pressure Safety Factors

Case	Location	Stress Conditions	Ultimate Pressure Limit		Safety Factor
			Psi	MPa	
1	Rotating shaft, thin-wall section	Hoop	49,893	344	34
2	Housing, large-diameter section	Hoop	45,833	316	31.3
3	Housing, small-diameter section	Hoop	36,932	255	25.2
4	Retainer cap bolts	Tensile	7,846	54.1	5.4
5	Retainer cap, inside lip	Shear	49,360	340	33.7
6	Retainer cap, inside lip	Local comp.	20,923	144	14.3

SEAL MATERIALS

The dynamic seal is the most critical component of the rotary joint assembly. Material properties of interest for the seal include hardness, resistance to cold flow, low coefficient of friction, compatibility with candidate heat pipe fluids, and wear resistance.

Candidate Materials

The most feasible candidate materials for the rotating joint seal include pure TFE, carbon-impregnated TFE, Kel-F, Vespel, Mylar, and carbon graphite. Lead and gold were also identified as potential metallic seal materials that could be plated on a machined metallic seal. These materials were evaluated on the basis of physical properties, past usage experience, permeability, and compatibility with potential heat pipe fluids such as ammonia, ethane, methane, oxygen, nitrogen, neon, and hydrogen. General considerations such as seal geometry, machinability, wear, crystallinity, etc., were also taken into consideration.

Physical Properties

A list of physical properties of candidate seal materials was gathered from available literature and is tabulated in Table 2-4. Coefficient of friction data were determined experimentally by the subcontractor using the test set-up shown in Figure 2-4.

From past experience, pure TFE Teflon is known to cold-flow badly as a function of time and is somewhat difficult to machine. Filled TFE has less tendency to cold flow, is easier to machine, and has higher physical properties depending upon the filler material.

In general, the physical properties of Kel-F are exceptionally good for this application; however, crystallinity and a high coefficient of friction make this material somewhat questionable. The high strength of Vespel combined with a low coefficient of friction make this material an attractive choice for the heat pipe rotating joint, although it is harder than either Teflon or Kel-F. Mylar is available in sheet form (up to 0.025 cm), and is adaptable to "lip seal" applications for cryogenic conditions but is not available in forms suitable for the selected seal design. Carbon graphite has many interesting

Table 2-4. Physical Properties of Candidate Seal Materials

PROPERTY	TFE	TFE (15% GRAPHITE)	KEL-F	VESPEL	MYLAR	CARBON GRAPHITE	LEAD	GOLD
TENSILE								
STRENGTH (Mpa)	17.2/20.7	9.0/18.6	31	89.7	158/276	27.6	14.5	13.2
ELONGATION (%)	250/350	130/240	165	7/9	100	-	43	45
YIELD POINT (Mpa)	-	-	29.7	-	-	-	-	-
YIELD 0.2% (Mpa)	-	-	14.5	-	-	-	-	-
MODULUS (Mpa)	400	1,400	1,310	-	3,793	35,172	13,793	82,758
IMPACT*	160	136	192	53	-	-	534	-
FLEXURAL								
STRENGTH (Mpa)	NO BREAK	5.9	58.6	117	-	172	-	-
MODULUS (Mpa)	620	-	1,130	3,103	-	-	-	-
COMPRESSIVE								
STRENGTH (Mpa)	11.7	9.8/11.8	29.7	276	-	69.0	-	-
MODULUS (Mpa)	-	662/614	910	-	-	-	-	-
SHEAR STRENGTH (Mpa)	-	-	44	89.7	-	-	-	-
FRICTION								
STATIC (AMB)	.04	.14	.45	-	-	.21	-	-
STATIC (CRYO)	-	-	.17	-	-	-	-	-
DYNAMIC (AMB)	.04	.12	.32	.04/.09	-	.003	1.1	-

*N-m per cm of notch

METHOD - ANGLE OF REPOSE
UNIT LOADING - YIELD STRENGTH RANGE
TYPE OF FRICTION - END OF SLIDING - START OF STATIC
TYPE OF SURFACE - POLISHED STEEL - UNLUBRICATED
SURFACE FINISH - $\overset{20}{\sqrt{}}$ MAX

RESULTS

TRIAL	θ	C_f
1	5°	.044
2	4.5°	.039
3	4.5°	.039
4	4.5°	.039

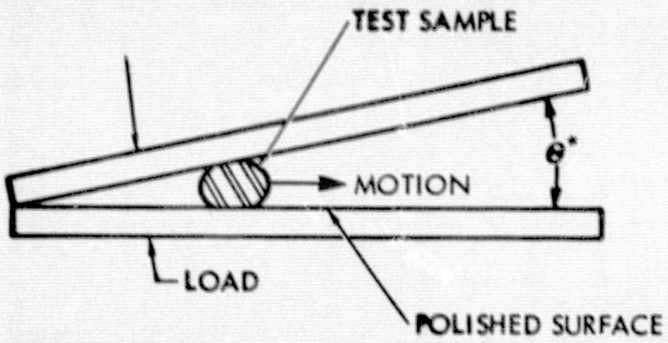

*ANGLE AT WHICH MOTION CEASES

SKETCH OF TEST METHOD

PROCEDURE:

1. INSERT SAMPLE BETWEEN PLATES TO DEPTH GREATER THAN EXPECTED ANGLE OF REPOSE
2. APPLY LOAD STEADILY UNTIL MOTION STOPS
3. MEASURE ANGLE BETWEEN BARS 1/2 OF ANGLE = ANGLE OF REPOSE
4. CLEAN AND RE-POLISH BARS AFTER EACH CHANGE OF MATERIAL

Figure 2-4. Coefficient of Friction Test Setup and Results

properties but its permeability to gases is unknown, which makes it somewhat questionable for this application. The only permeability data available were for Teflon and Kel-F, and are shown in Table 2-5.

Table 2-5. Permeability of Teflon and Kel-F to Various Gases at 77 K

Material	Permeability Rates × 10^{-7} scc/sec/cm^2/mm/atm			
	H_2	He	N_2	O_2
Teflon	18	530	2.4	7.6
Kel-F	0.74	-	0.0025	0.028

Leakage

Total external leakage from the heat pipe coupling will be that from the static seal plus the dynamic shaft seal and, under ideal conditions, will be limited by permeability through the plastic seal material. Microscopic sealing surface irregularities as a result of lapping and polishing operations, as well as slight eccentricities between the shaft and seal, will contribute to additional leakage.

If the leakage across the seal interface is sufficiently low after wear-in, the leakage will approach a limit which is equal to the permeability of the seal material.

Permeability of Kel-F and Teflon to various gases at 293 K is shown in Table 2-5. It should be noted that Teflon data for thin-film Teflon and the permeability of the graphite impregnated seal may be significantly different. It is also likely that the permeability will vary with temperature, although data at cryogenic temperatures were unavailable.

Order-of-magnitude leakage rates were computed from the data in Tables 2-4 and 2-5, based on the seal cross-sectional area and for the design pressures at ambient and LN_2 temperature. Resulting leakage rates for Kel-F and Teflon are shown in Table 2-6.

As shown in Table 2-6, helium leakage rates with Teflon are significantly higher than the 1×10^{-6} sccs design goal. Kel-F data are expected to be significantly better. Helium leakage data for Kel-F are estimated by assuming that

the ratio of the permeability to helium compared to hydrogen is the same for Kel-F as for Teflon. Leakage due to permeability with Vespel is expected to be considerably less due to the structure of the material, although no permeability data could be located.

Table 2-6. Projected Leakage Estimates

	Leakage (sccs)			
	P = 10.1 MPa (99.6 atm) T = 293 K		P = 0.4 MPa (3.95 atm) T = 77 K	
Gas	Teflon	Kel-F	Teflon	Kel-F
H_2	1.1×10^{-4}	4.5×10^{-6}	4.3×10^{-6}	1.8×10^{-7}
He	3.2×10^{-3}	1.3×10^{-4}*	1.3×10^{-4}	$5.2\ 10^{-6}$*
N_2	1.5×10^{-5}	1.5×10^{-8}	5.8×10^{-7}	6.0×10^{-10}
O_2	4.6×10^{-5}	1.7×10^{-7}	1.8×10^{-6}	6.7×10^{-9}
*Estimated				

Torque

Torque will primarily be a function of the coefficient of friction between the dynamic seal and the rotating shaft. This will be affected by the spring loading imposed on the seal due to the 16 helical compression springs as well as the surface finish of the seal and its mating interface. In general, it is expected that the shaft torque and external leakage will be inversely proportional, and that torque will be a maximum when shaft seal leakage is minimum.

The 16 helical compression springs have a spring constant of 89 N/cm (50.8 lb_f/in.). At the nominal compression (15.5% of the free length), the compressive load on each spring is 42.7 N (2.4 lb_f). The net load transferred radially inward to the dynamic sealing surface is 121 N (27.2 lb_f). In addition to the spring load, the internal pressure causes an additional loading on the seal against the rotating shaft. The additional load is 5.1 N (1.1 lb_f) at 0.4 MPa, and 128 N (28.8 lb_f) at 10.1 MPa. Coefficient of friction data and calculated torque values for the ambient and cryogenic pressure conditions are summarized in Table 2-7. For Kel-F, the calculated torque is 0.2 N-m at 0.4 MPa, and 0.76 N-m at 10.1 MPa, compared to the design requirement of 3-5 N-m.

Table 2-7. Calculated Torque Values

Material	Coefficient of Friction		Torque (N-m)	
	77 K	293 K	0.4 MPa	10.1 MPa
Kel-F	0.17	0.32	0.2	0.76
Vespel	0.04*	0.09	0.05	0.21
Teflon/graphite	0.1*	0.12	0.12	0.28
*Estimated				

Selected Seal Material

Based on the data presented in Tables 2-4 through 2-7, and from extensive cryogenic valve experience on the Saturn S-II vehicle, it would appear that Kel-F, Vespel, and graphite-impregnated TFE would all be potentially good seal materials. Both Kel-F and Vespel have good compressive strengths coupled with reasonably good coefficients of friction. Graphite-impregnated Teflon has the most desirable properties except for permeability. Because of the limited scope of this program, only one seal material could be tested. Kel-F was selected as the baseline seal material, although spare seals of Vespel and graphite/Teflon were purchased for potential future use.

FABRICATION AND ASSEMBLY

The rotary joint test fixture was fabricated under subcontract by the Rudolph E. Krueger Company, Newport Beach, California. The shaft, housing, wedge ring, and diaphragm washer were machined from heat-treated 17-4 stainless steel. The sealing surfaces on the shaft and the diaphragm washer were ground, hard chrome-plated, and polished to a surface roughness of less than three helium light bands. The thrust bearing and inside bearings were commercially purchased aircraft quality bearing assemblies (with no lubricant). The dynamic seals were fabricated to specification by Thermec Engineering Company of Anaheim, California. The static "K" seal was supplied by Sierracin/ Harrison Corporation, Burbank, California (PN 12195CR1437).

The assembled rotary joint test fixture is shown in Figure 2-5. Figure 2-6 shows the unit disassembled with the internal components.

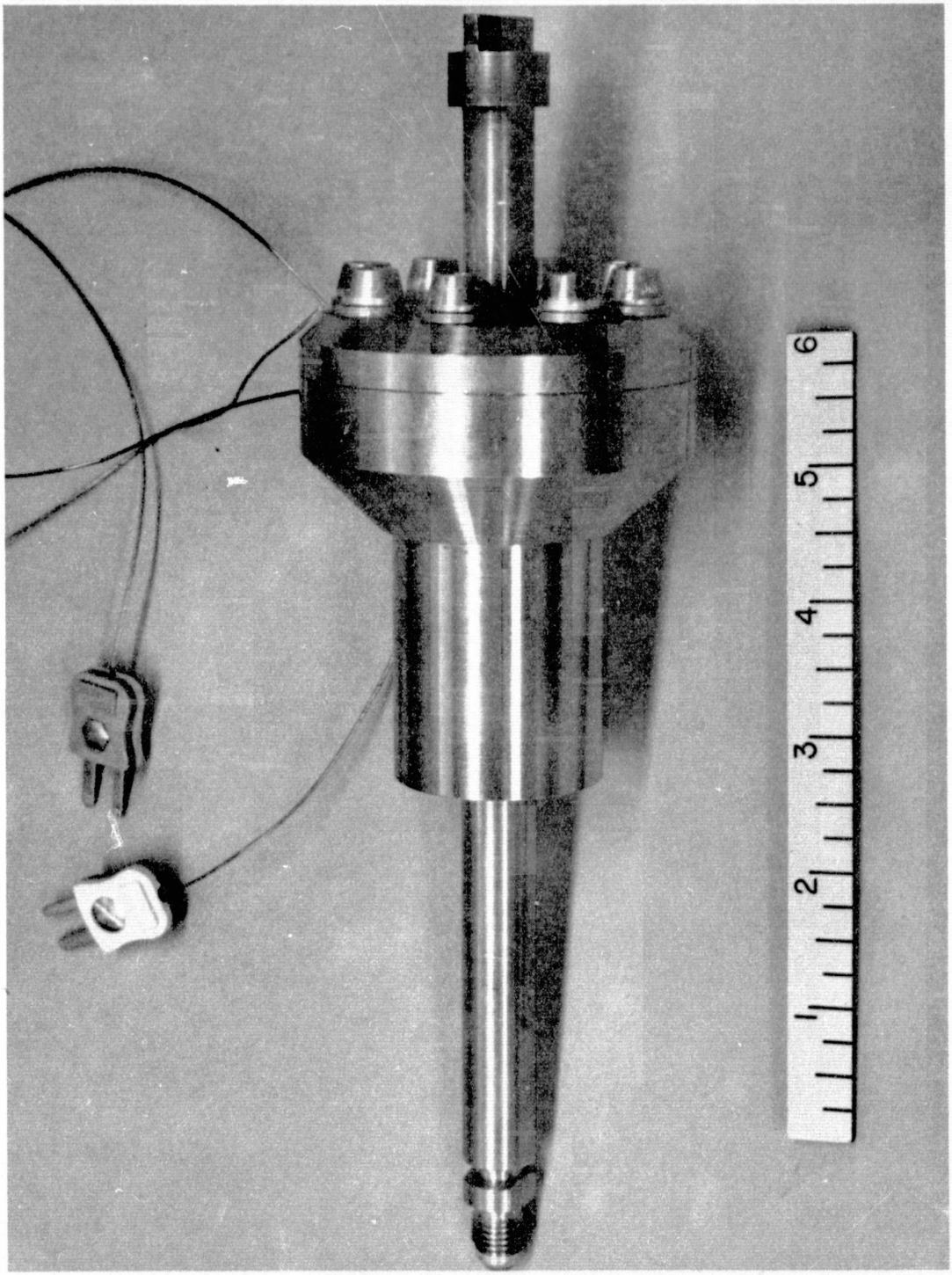

Figure 2-5. Assembled Rotary Seal Device

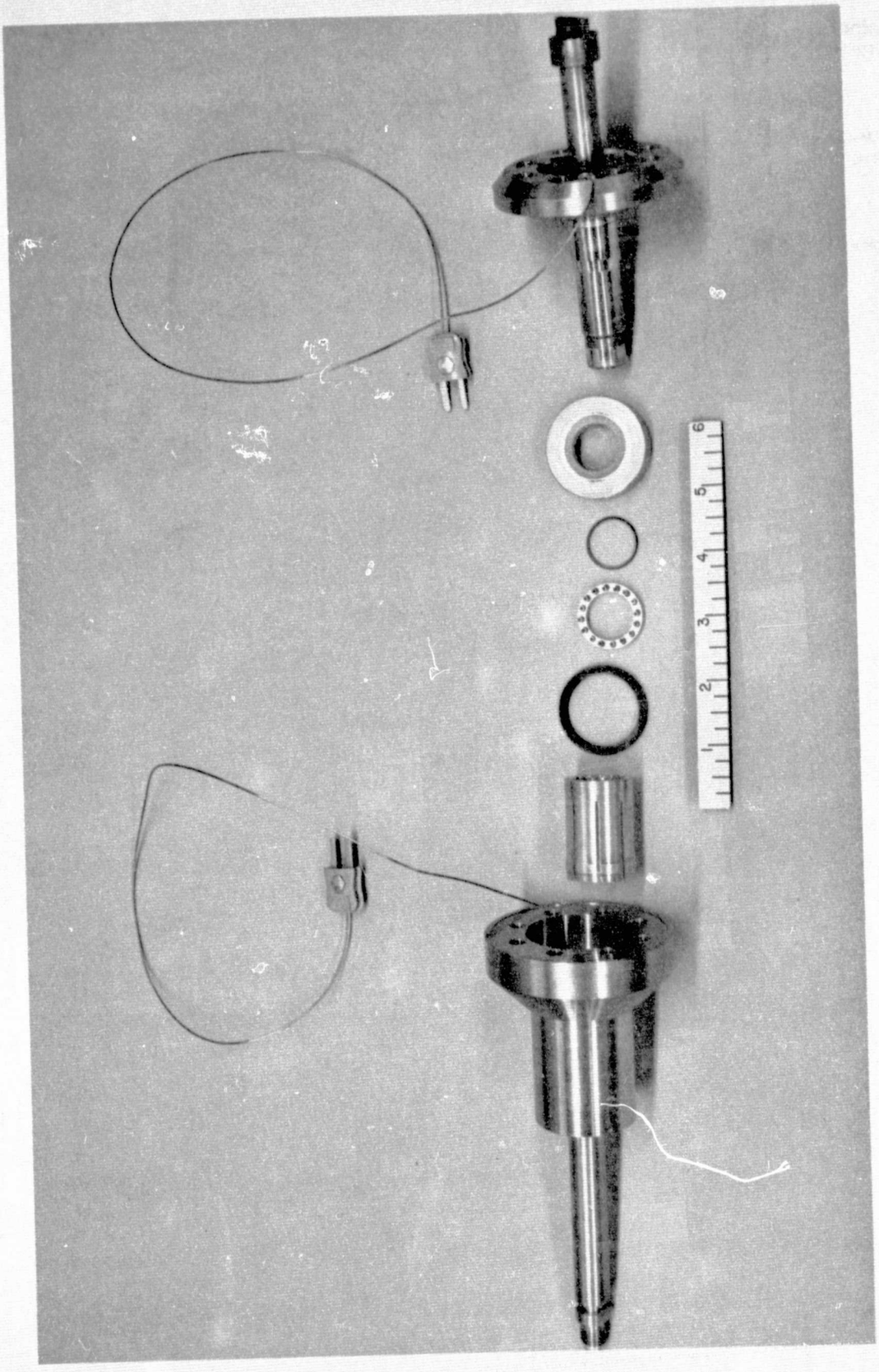

Figure 2-6. Exploded View of Rotary Seal Assembly

Cleaning

Prior to leak-testing with the Kel-F seals, the test article was disassembled and carefully cleaned. All components except the seals were vapor-degreased, and then immersed in a hot solution of Turco 4090 in an ultrasonic bath. The items were rinsed with hot tap water and deionized water and finally dried in an oven. Reassembly was accomplished on a laminar flow bench. The article was assembled with a Vespel dynamic seal and unlubricated "K-seal" for the purpose of pressure proof testing. The 1/4-28 assembly bolts were tightened to a torque of 10 N-m.

Proof Pressure Testing

The test article, protected with a Millipore filter, was then pressurized to 20.2 MPa with nitrogen gas. Leakage was evident, but no distortion of the housing was noted. As a preliminary leak check, the assembly was pressurized to 9.9 MPa with helium. A pressure decay of 0.28 MPa in five minutes was observed. A soap solution test revealed leaking gas originating from behind the exposed ball bearings, as would be expected.

Final Assembly

The Millipore filter was removed from the test article, which was then disassembled on the laminar flow bench. All components were rinsed with Freon TF and dried with a stream of filtered nitrogen gas. The test article was then reassembled with one of the Kel-F dynamic seals. The "K-seal" was coated with a light layer of Celvacene high vacuum grease for lubrication and to minimize the possibility of its leaking, since the performance of the dynamic seal was of principal interest.

LEAK TEST PROGRAM

A series of tests were run to determine the performance of the rotating joint assembly with the Kel-F seal under varying conditions. The test set-up, leakage measurement tèchnique, test procedures, and results are described below.

Test Set-Up

The test system, pictured schematically in Figure 2-7, consists of four sections: (1) the test article helium pressurization system, (2) the vacuum

Figure 2-7. Leak Test System Schematic

system, (3) the sensitivity calibrator, and (4) the leak detector. The helium pressurization system was designed to provide pressurization up to 0.6 MPa, to within ±3.4 Pa, or up to 11 MPa to within ±0.14 MPa. An 8-μm Millipore filter is situated between the pressurization system and the test article. The test article and connecting line can be evacuated with the mechanical pump provided.

The vacuum system consists of a portable 10.2-cm (4-in.) diffusion pump with a 45.7-cm (18-in.) diameter feedthrough collar and bell jar assembled on the baseplate. The sensitivity calibrator is a Veeco standard leak ($Q \simeq 1\times10^{-4}$ atm cm^3/sec) pressurized with helium. A sintered metal in-line filter is inserted between the leak and the helium supply, while an isolation valve is interposed between the leak and the vacuum chamber.

The leak detector used was a CEC Type 24-120A with Type 24-038 Test Port and Roughing Station. Figure 2-8 is a photograph of the assembled apparatus.

The physical test arrangement is shown schematically in Figure 2-9, while Figure 2-10 gives a photographic view. The rotary seal test article was mounted rigidly on a 45.7-cm-diameter feedthrough collar, between diagonally opposite feedthrough ports. At one end the shaft was attached to a low-speed rotational drive, while the other end was connected to the helium pressurization line. A liquid-cooled brass collar, which was fitted around the body of the test article, provided for cooling the housing to 80 K. DC340 heat transfer compound was used at the interface to enhance the heat transfer, which would otherwise have been poor in vacuum. Two AWG No. 30 chromel-constantan (Type E) thermocouples were attached to the test article housing at the locations indicated in the schematic. As shown in the photograph, the specimen was supported off the baseplate in such a way as to minimize heat input by conduction. Although not shown, in the actual testing multi-layer insulation would have been wrapped around the exposed portion of the test article housing, also to minimize heat input.

Leakage Measurement

Test article leak rate determinations were accomplished under simulated usage conditions with a mass spectrometer-type helium leak detector. This was used to sample the atmosphere in an evacuated bell jar containing the

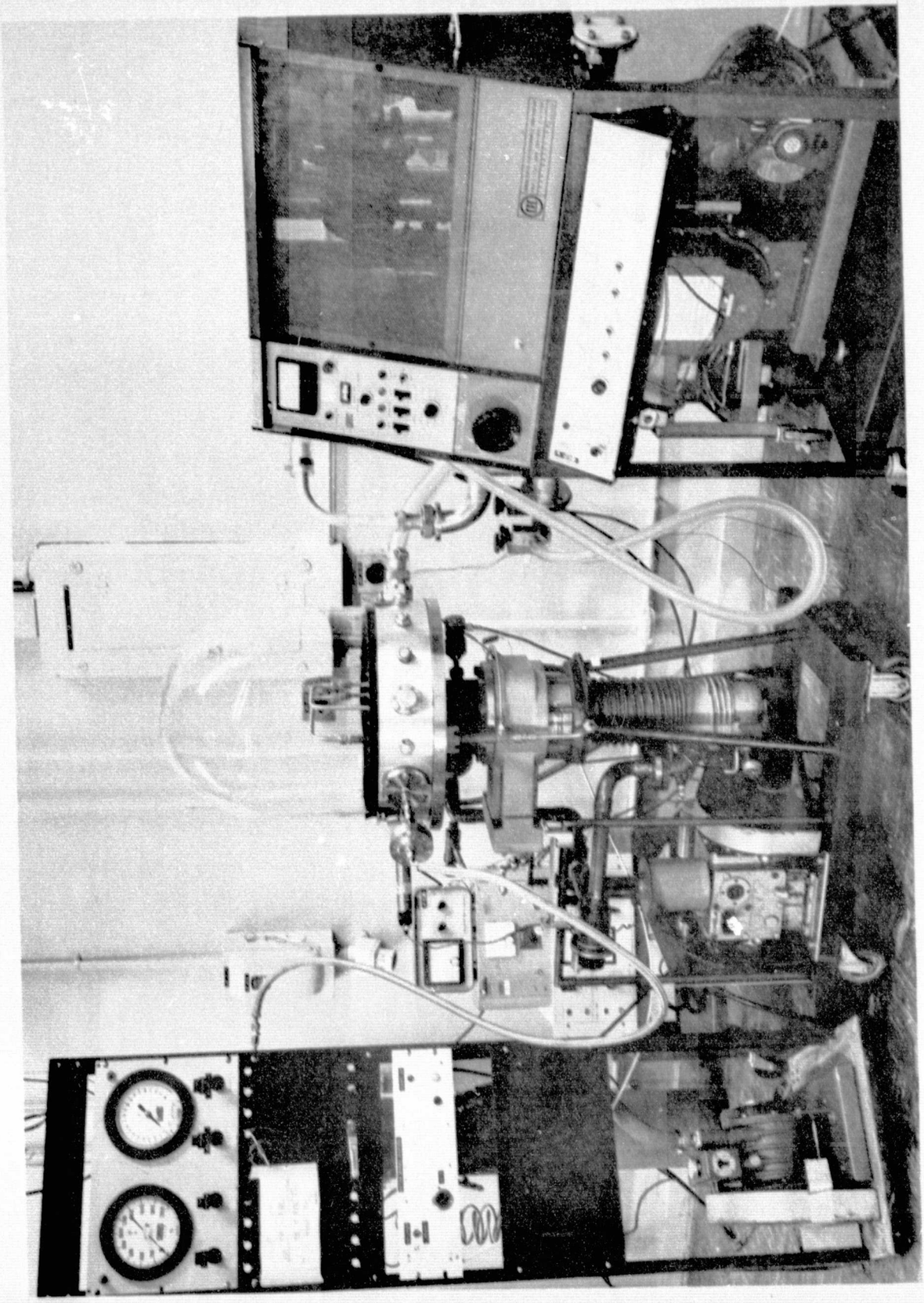

Figure 2-8. Leak Test System

Figure 2-9. Test Setup Schematic

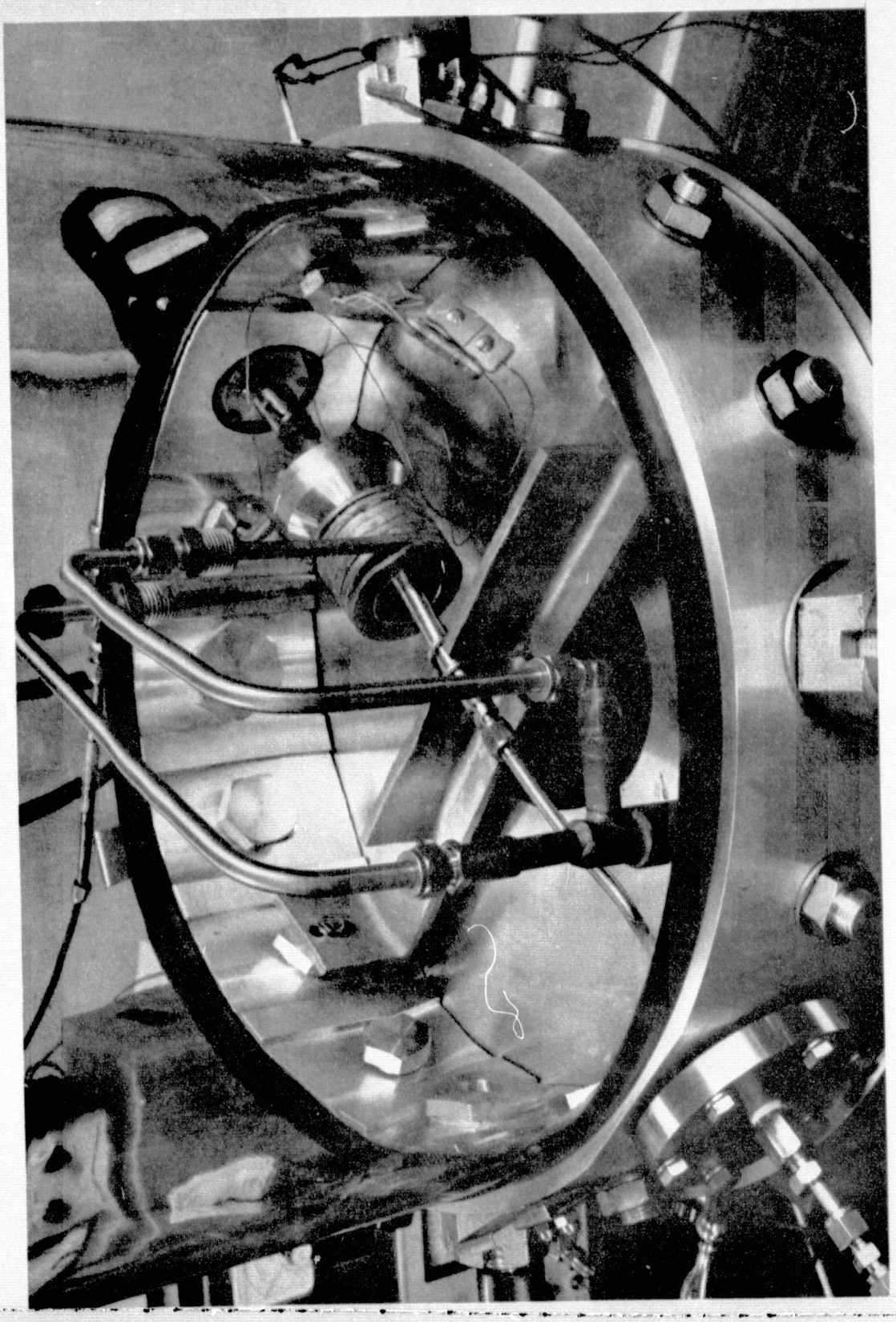

Figure 2-10. Test Fixture

pressurized test article. A sensitivity calibrator (standard leak) was installed with its outlet situated in close proximity to the shaft end of the test article. The purpose was to establish the sensitivity of the leak detector under the same conditions which would exist when determining the test article leakage.

Calibration of Standard Leak

The Veeco standard leak used as the sensitivity calibrator had to be itself calibrated since its nominal value was questionable and the inlet pressure for which this value was appropriate was not indicated. Since the operating condition (i.e., leakage into an evacuated volume) was expected to influence the leak rate, calibration under similar conditions was desirable. This was accomplished by a chromatographic accumulation method, described below.

The set-up is shown schematically in Figure 2-11. The Hoke bottle and connecting lines up to the leak tube orifice were evacuated and isolated from the vacuum pump. The helium regulator and bleed valve were then adjusted to provide the desired pressure and the time noted. After an appropriate interval, the Hoke bottle was valved off and removed from the leak. The bottle was then filled to 0.21 MPa with GN_2 and the contents analyzed with the gas chromatograph to determine the mole fraction (N) of helium present. This is related to the leak rate by the following expression:

$$Q_{sc}(\text{atm cm}^3/\text{sec}) = N \times V \times \left(\frac{30}{14.7}\right) \times \left(\frac{1}{\theta}\right)$$

where

V = Hoke bottle volume, cm^3
θ = Time, sec

The leak rate was determine for the two inlet pressures of interest, with the following results:

Pressure (MPa)	Q_{sc}, atm cm^3/sec
0.13	1.7×10^{-4}
0.20	3.1×10^{-4}

Figure 2-11. Standard Leak Calibration Test Setup Schematic

Vacuum Decay Technique

In the event that it became apparent the test article leakage was too great to be measured with the helium leak detector, the leak rate test procedure was modified to obtain an approximate air leak rate (0.1 MPa pressurization) by observation of the bell jar pressure rise.

With the valve to the sensitivity calibrator closed, the bell jar was evacuated with the 10.2-cm diffusion pump system. Simultaneously, the test article was evacuated with the mechanical pump provided. The evacuated test article was isolated from its pump, and the main slide valve closed. The basic bell jar vacuum decay rate was observed. This represents inleakage and outgassing.

The valve isolating the sensitivity calibrator was then opened, as was the slide valve. After the system pressure dropped to below 1×10^{-5} torr, the slide valve was closed and the pressure rise again observed. This represents the calibrator leak rate plus inleakage and outgassing.

The sensitivity calibrator was then isolated from the bell jar, the test article pressurization line vented to atmosphere, and the slide valve again reopened. After achieving $P < 1\times10^{-5}$ torr, the slide valve was closed and the pressure rise noted. This represents the test article leak rate and system inleakage plus outgassing.

If the system volume is known, the leak rate is readily calculated from the relation

$$Q = 5.98\times10^{-3}\left(\frac{dP}{d\theta}\right)\left(\frac{V}{T}\right) \text{ atm cm}^3/\text{sec}$$

where

$\left(\frac{dP}{d\theta}\right)$ = decay rate, μtorr/min.

V = volume, liters

T = absolute temperature, K

The system volume was estimated as 80 liters. Based on the decay rate observed for the sensitivity calibrator, whose leak rate for air into vacuum was 1×10^{-3} atm cm^3/sec, the chamber volume was determined to be 108 liters. An average value of V = 95 liters was used in calculating the test article leak rate.

Test Procedure

After each set-up, before the bell jar was put in place, the coolant lines and test article were pressurized to about 15 psig with helium and all connections were checked with the leak detector using the sample probe. If this test proved negative, the bell jar was installed and evacuated using the leak detector auxiliary roughing pump. At the same time, the test article was evacuated with the other mechanical pump. It was then determined if the primary leak detector vacuum system could handle the bell jar leakage and outgassing with or without assistance from the auxiliary roughing pump. The feedthrough collar was then leak-checked by spraying helium around the feedthroughs and the bell jar seal. The coolant line was again pressurized with helium for a more sensitive indication of leaks at the fittings. If the preliminary system leak checks proved satisfactory, the leak rate testing could proceed.

The leak detector throttle and roughing valves were closed and the slide valve to the 10.2-cm diffusion pump system opened. The system pressure was reduced to $P < 1\times10^{-5}$ torr prior to leak rate testing. The leak detector background reading (M1) was noted and the roughing valve between the mechanical pump and the test article was closed. The throttle valve was then opened fully and the bell jar background reading (M2) noted. The throttle valve was again closed, after which the valve isolating the sensitivity calibrator was opened. After the initial helium pressure surge had been reduced by the 10.2-cm (4-in) diffusion pump, the throttle valve was again fully opened and the meter reading (M3) observed after equilibration. The leak test system sensitivity is found from the expression

$$S = \frac{Q_{sc}}{(M3-M2)}$$

Where S = sensitivity, atm cm^3/sec div.

Q_{sc} = leak rate of sensitivity calibrator, atm cm^3/sec

M = meter reading, divisions

The throttle valve was again closed, the sensitivity calibrator isolated from the bell jar, and the desired helium pressure applied to the test article. The throttle valve was opened and the meter reading (M4) noted. The test article leak rate was obtained from the relation

$$Q = (M4-M2) \times S$$

The above procedure was used for all leak rate testing except where the leak rate of the test article exceeded the effective range of the leak detector. In these few instances, the air leak rate was determined by the vacuum decay technique.

Test Results and Observations

When the assembly was tested statically with the first Kel-F seal installed, a disappointingly high leak rate at low helium pressures was observed (see Figure 2-12). The decision was made to proceed with the wear-in in hopes it would improve the seal performance. The wear-in consisted of 10,000 revolutions at 5 rpm with the assembly at atmospheric pressure, internal and external. The shaft was rotated counterclockwise as viewed from the drive end. After wear-in was completed, it became evident as soon as the leak test procedure was initiated that the leakage had increased considerably. The leak rate for air was determined by the vacuum decay technique, and the test article was removed from the fixture, disassembled and inspected with a low-power stereoscopic microscope. Severe wear of the surface of the Kel-F seal was noted as shown in Figures 2-13 and 2-14. Numerous flakes of Kel-F were adhering to the shaft. One of them contained a flake of metal which may have been from the chromium plating. Smear markings were observed on the shaft and load bearing ring (see Figures 2-15 and 2-16). The shaft was returned to R. Krueger Company for polishing to remove the smear marks.

The test article was cleaned and reassembled with the second Kel-F seal and repolished shaft. The initial static leak determination was surprising in that the leakage was significantly lower than it had been for the previously tested seal (Figure 2-18). The reduction was felt to be due to the smoother surface of the shaft after repolishing.

It was decided to wear-in the second Kel-F seal at a rate of only 4 rev/hr, with leak rate determinations during the wear-in while the shaft was rotating. The wear-in was interrupted after 5 and 25 revolutions to permit static leak rate determinations. Although leakage was higher when the shaft was rotating, static leakage after five cycles of wear-in had increased only slightly over values obtained prior to wear-in. Interestingly, leakage at all pressures was greatly reduced when the static test was repeated, indicating

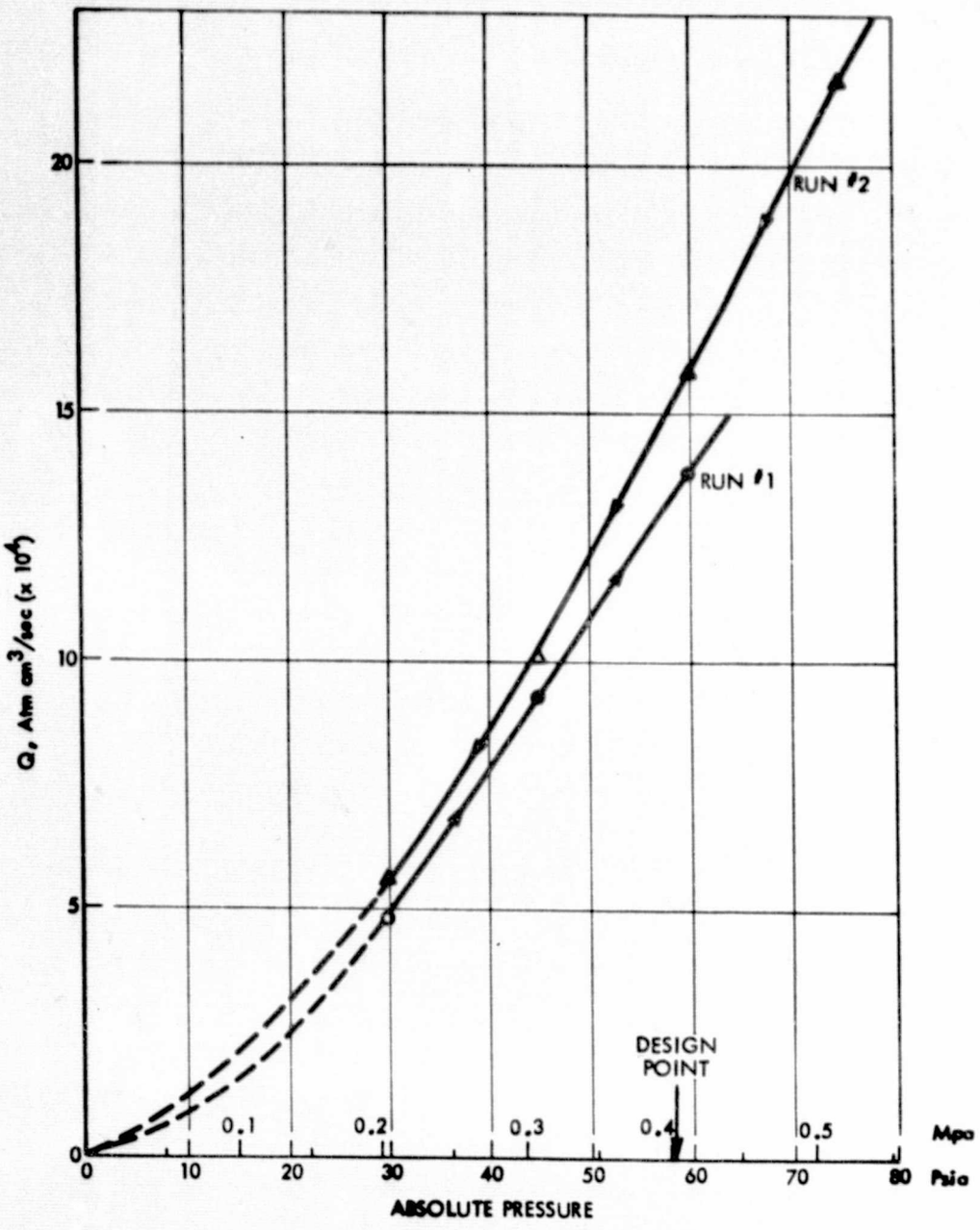

Figure 2-12. Helium Leak Rate vs. Pressure, Kel-F Seal No. 1, As-Received Condition

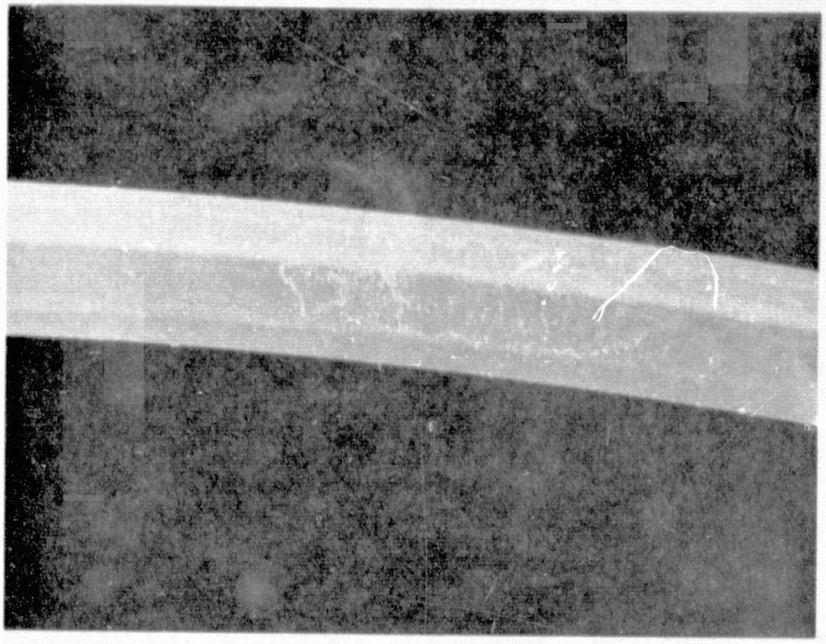

Figure 2-13 - Kel-F Seal Specimen No. 1 After Wear-in (20X)

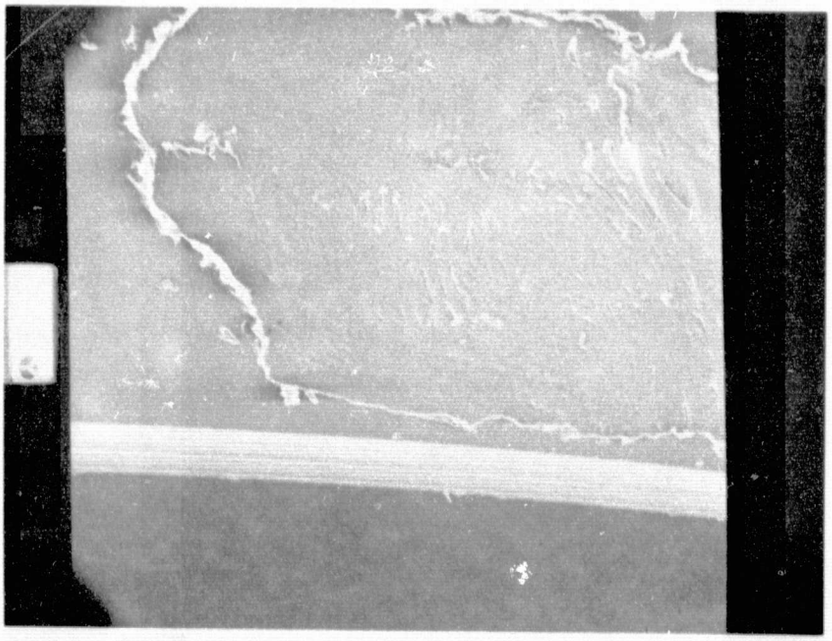

Figure 2-14 - Kel-F Seal Specimen No. 1 After Wear-in (110X)

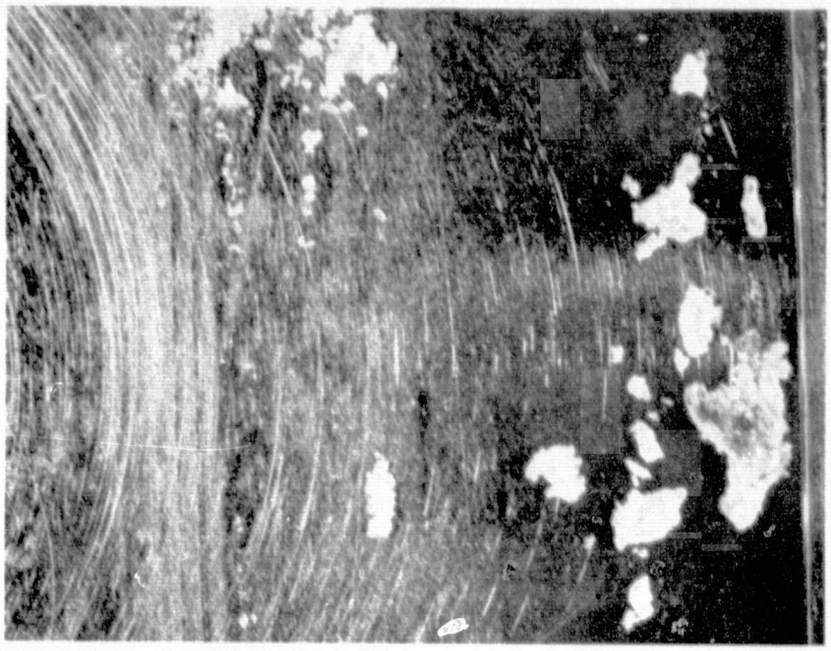

Figure 2-15. Shaft Seal Surface After Wear-in (20X)

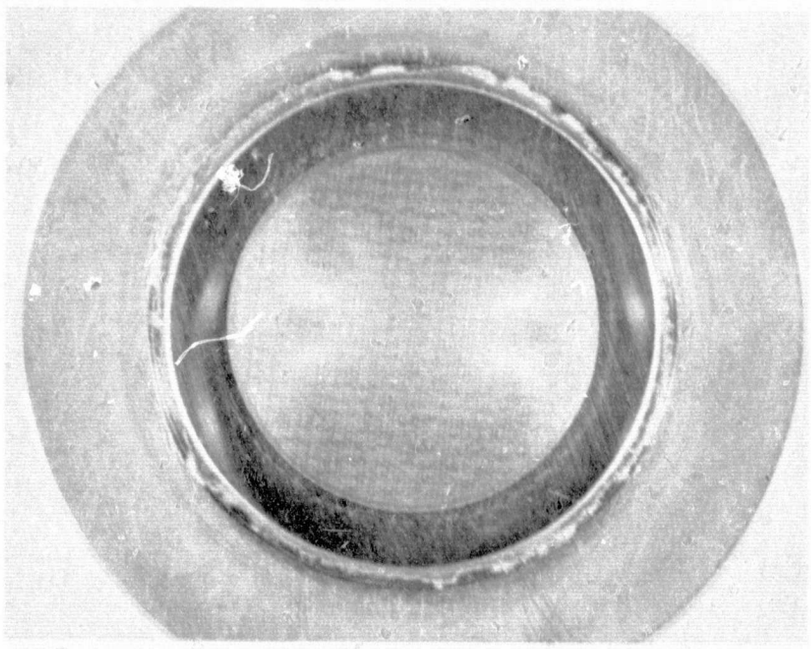

Figure 2-16. Load Bearing Ring Seal Face After Wear-in (2.5X)

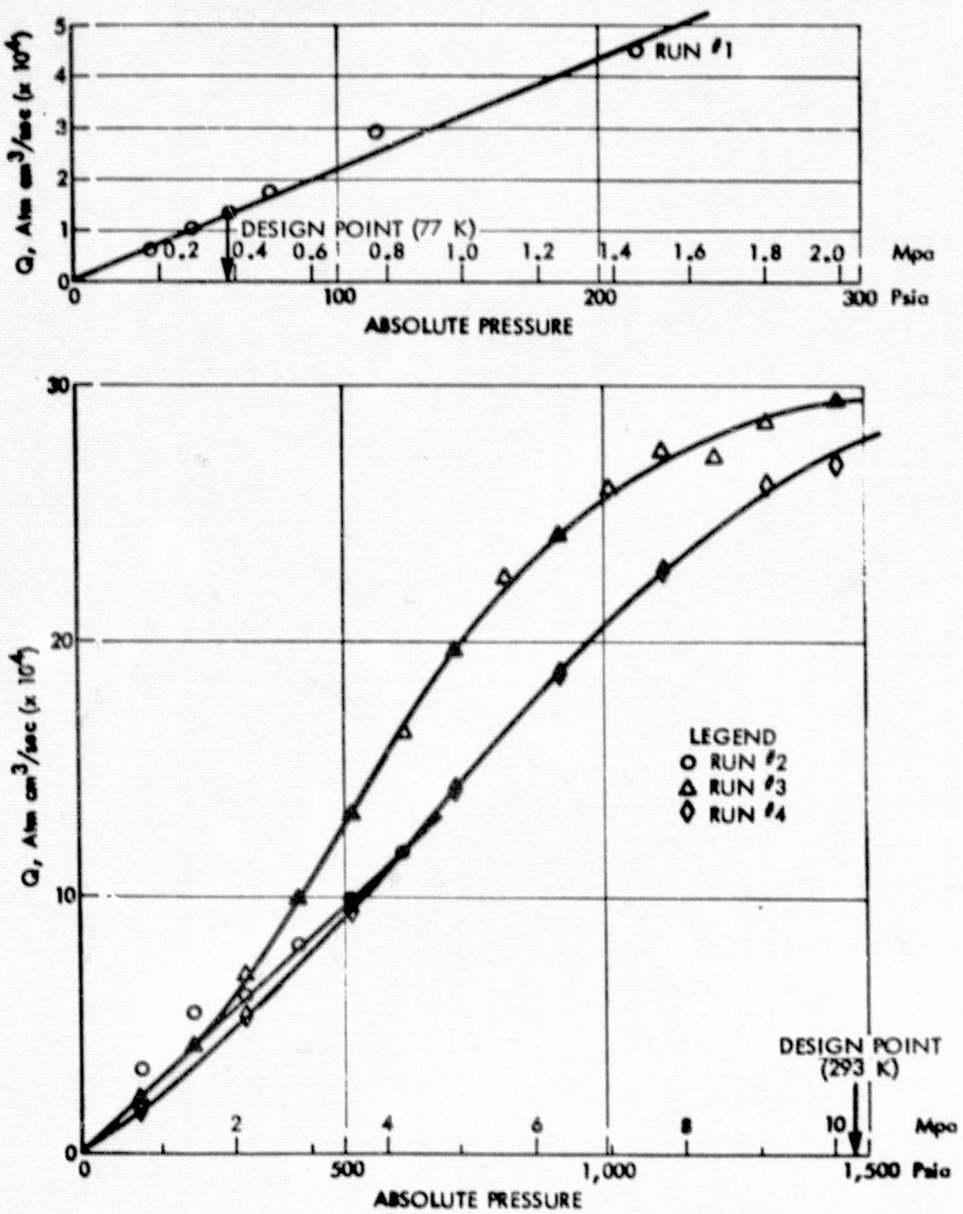

Figure 2-17. Helium Leak Rate vs. Pressure Kel-F
Seal No. 2, As-Received Condition

an effect of pressure cycle (see Figure 2-18). On continuation of wear-in, dynamic leak rates were correspondingly lower, but showed some increase as wear-in continued. Static values, however, reached their lowest values after 25 revolutions (Figure 2-19). Wear-in was continued and a high dynamic leak rate was observed after 42 cycles, indicating seal failure. Shaft rotation was terminated, whereupon a similarly high leak rate was observed for the static condition.

The test article was again removed from the test fixture for inspection. After disassembly, wear of the Kel-F seal was confirmed, with flakes of Kel-F adhering to the seal surface. The condition was not as severe as had been noted in the case of the first seal tested. No damage to the shaft was noted.

A new shaft was fabricated using a harder steel in hopes of obtaining a smoother shaft surface for the seal to wear against. Discussions were also held with Thermec Engineering Company, the supplier of the Kel-F seals. The wear problem was felt to be due to the amorphous Kel-F which was used for the seals. While the amorphous material is better than the crystalline material in terms of ductility at cryogenic temperature, it apparently is much less wear-resistant. Previous experience with static seals on the Saturn II program indicated that better and more reliable seal performance was achieved at cryogenic temperatures with the amorphous rather than the crystalline seal material. It is possible that some intermediate level or percentage of crystallinity in the Kel-F material would provide acceptable leakage as well as good wear resistance. Because of the limited scope of this effort, additional materials were not evaluated during the program.

Additional testing and evaluation were performed using this seal test fixture under independent research and development at Rockwell. Results of this effort are described in Reference 3. A graphite-impregnated Teflon seal was tested under the same conditions as the Kel-F seal. Static leakage was measured as a function of pressure prior to wear-in. As shown in Table 2-8, the static leakage rates were somewhat lower than the initial values for the Kel-F seal. A slow wear-in consisting of 400 cycles at 4 rev/hr was performed, after which static leakage was rechecked. Results showed that leakage had improved significantly. The joint was then cooled to 100 K and the dynamic leakage was measured at a rotation rate of 4 rev/hr. Results are shown in Table 2-9.

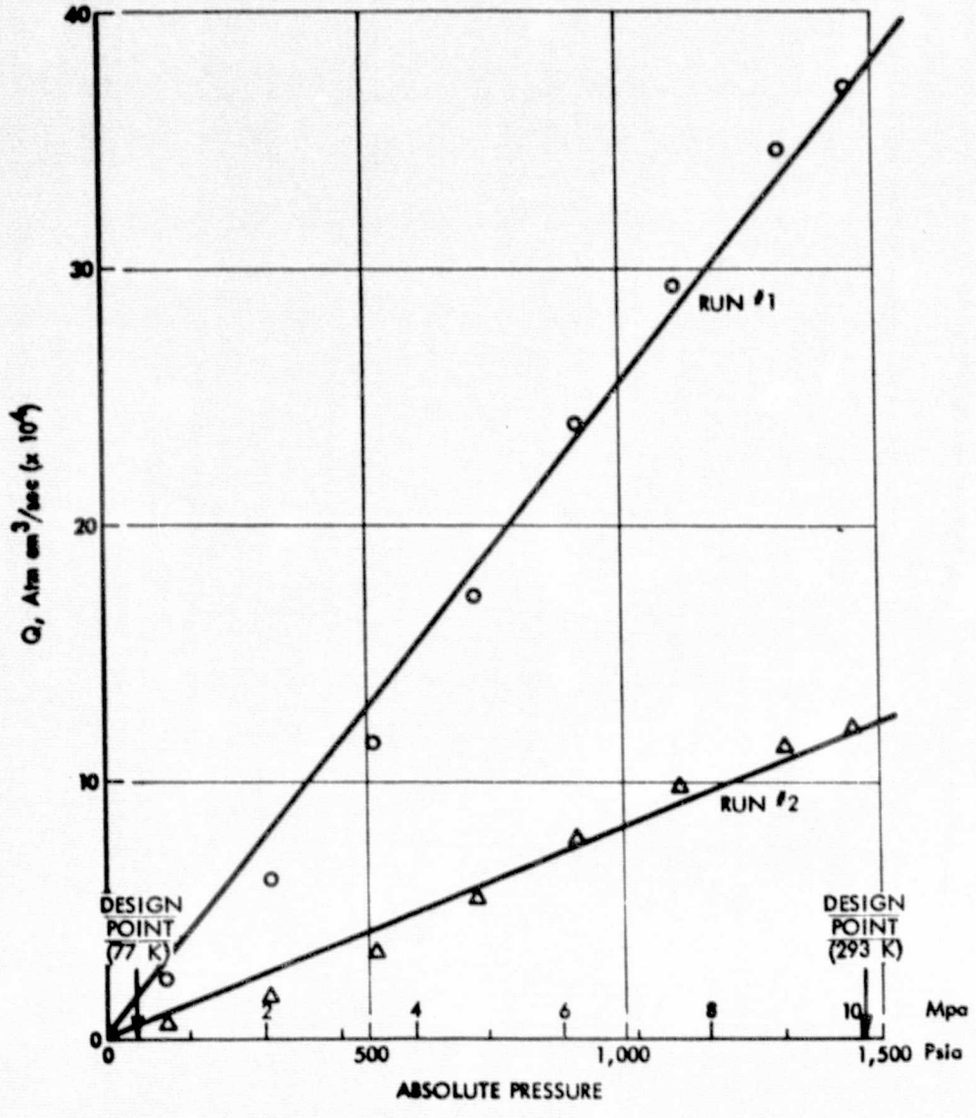

Figure 2-18. Static Helium Leak Rate vs. Pressure Kel-F Seal No. 2 After 5 Cycles Wear-in at 4 rph

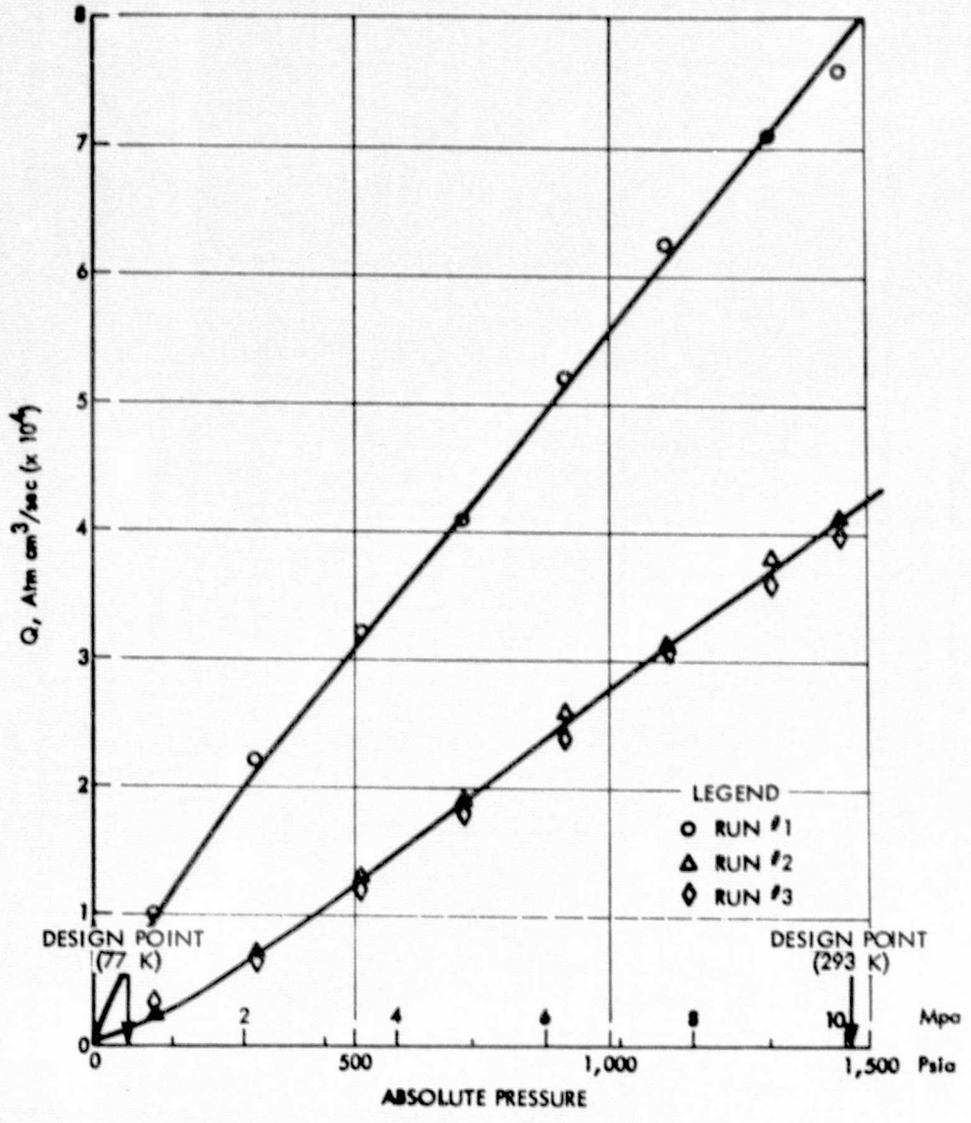

Figure 2-19. Static Helium Leak Rate vs. Pressure Kel-F Seal No. 2 After 25 Cycles Wear-in at 4 rph

Table 2-8. Summary of Helium Leak Rate Data—Teflon/Graphite Seal No. 2

Test No.	Description of Test	Sensitivity atm-cm^3/sec-div.	Leakage, atm-cm^3/sec ($\times 10^3$) at P, MPa					
			0.1	0.21	0.69	3.15	6.21	9.9
1	Static, initial	5.5×10^{-8}	3.6	-	-	-	-	-
2	Dynamic, 4 rev/hr after 2 rev	5.5×10^{-8}	1.3	-	-	-	-	-
3	Dynamic, 4 rev/hr after 6 rev	5.6×10^{-8}	1.1	-	-	-	-	-
4	Dynamic, 4 rev/hr after 10 rev	5.0×10^{-8}	1.6	-	-	-	-	-
5	Static, after 10 rev wear-in	5.2×10^{-8}	0.9	-	-	-	-	-
6	Dynamic, 4 rev/hr after 400 rev	2.4×10^{-7}	0.03	0.06	-	-	-	-
7	Static, after 400 rev wear-in	8.0×10^{-8}	0.02	-	0.08	0.09	0.16	0.25
8	Repeat	7.3×10^{-8}	-	-	0.10	0.08	0.16	0.20 (0.25)*
9	Repeat, 2 days later	1.8×10^{-7}	-	-	0.09	0.05 (0.07)*	0.09 (0.11)*	0.16 (0.20)*

*Equilibrium

Table 2-9. Summary of Helium Leak Rate Data—Teflon/Graphite Seal No. 2 (Incl. Cryogenic)

Test No.	Description of Test	Sensitivity atm-cm^3/sec-div.	Leakage, atm-cm^3/sec ($\times 10^3$) at P, MPa				
			0.4	0.69	3.45	6.21	9.9
10	Repeat, 4 days later	3.3×10^{-7}	-	0.09 (0.10)*	-	-	0.09 (0.35)*
11	Static, at temp. indicated	3.3×10^{-7}	25.8 (115 K)	-	-	-	-
12	Dynamic, at temp. indicated, after <1 rev	3.3×10^{-7}	16.6 (105 K)	-	-	-	-
13	Dynamic, at temp. indicated, after ~1 rev	1.8×10^{-7}	9.0 (105 K)	-	-	-	-
14	Static, after cold cycle (R.T.)	3.5×10^{-7}	-	0.06	0.08	0.15	0.28 (0.32)*
15	Dynamic, at temp. indicated	3.1×10^{-7}	0.24 (299 K) 0.24 (268 K) 0.34 (229 K) 1.8 (208 K) 2.1 (195 K) 2.9 (184 K) 5.1 (174 K) 11.5 (166 K) 14.6 (155 K)				

*Equilibrium

Rotational Torque

The rotational torque with the Kel-F seal was approximately 0.6 N-m at ambient temperature, although the static break-away torque was about twice this high. At cryogenic temperature, the torque was affected by the rotational feedthrough to the vacuum bell jar. From the coefficient of friction data in Table 2-7, the torque at cryogenic temperature is estimated to be approximately 2 N-m, still below the 3-5 N-m design goal. With the Teflon/graphite seal, the turning torque was considerably less. At ambient temperature, the torque was approximately 0.1 N-m. Under cryogenic operating conditions and 0.4 Mpa pressure, the torque increased to 0.55 N-m.

Discussion of Results

The tenfold difference in as-received static leak rates between the two Kel-F dynamic seals tested is difficult to explain. The only significant difference between the two set-ups and tests was that the shaft had been reworked in the interim. This rework amounted to simply polishing the shaft to remove the smear marks produced by wear-in of the first seal tested. It is, of course, possible that the first seal had a defect that was not discovered in the pre-test inspection.

Wear-in of the seals in both instances led to failure, catastrophic in the first case where a relatively high rate of 5 rev/min. was used for a total of 10,000 cycles. In the second test, wear-in at a much slower rate (4 rev/hr) led initially to some improvement in seal performance, but after only 42 cycles resulted also in failure. Failure in both instances appeared to be due to the tearing away of material from the Kel-F surface, as evidenced by the photographs in Figures 2-14 and 2-15.

As would be expected, dynamic leak rates (i.e., determined while shaft was rotating) were usually higher than rates determined for the static condition prior to wear-in. Static values after wear-in indicated improvement in some instances, as previously described. Unexpected was an observed improvement in seal performance, apparently the result of simple pressure cycling in the course of leak testing at high helium pressures.

This was observed with the second seal after wear-in, but was not evident in the as-received condition. The best seal performance obtained was for the second seal specimen after 25 cycles wear-in at 4 rev/hr. Static leak values of 2×10^{-5} atm-cm^3/sec at 0.69 MPa, and 4×10^{-4} atm-cm^3/sec at 9.9 MPa were observed. This seems to offer some promise of achieving the design goal leakage with this seal concept, perhaps with a different seal material, or by control of the fit or compression of the seal against the shaft.

3.0 ROTATING WICK DEVELOPMENT PROGRAM

In addition to the rotating container, a rotating heat pipe requires a wicking system which is capable of transporting the working fluid across the rotating interface. A separate development program was undertaken to develop a wick with a rotating interface, and to evaluate its performance in terms of self-priming and capillary pumping capability. The requirements for a rotatable wick are discussed below. The subsequent sections describe the design, fabrication, and testing of a wicking system for a rotatable heat pipe.

REQUIREMENTS

The primary requirements for a rotating wick are continuity across the rotating interface, and compatibility with the working fluid. In addition, the wick must meet the capillary pumping and flow permeability requirements dictated by the application, and the wick must be able to self-prime from a dry condition in a 1-g gravity field. The wicking system must also allow sufficient space for the transport of the vapor across the rotating interface.

ROTATING WICK CONCEPT

A rotating wick concept was designed based on the spiral multiwrap wick design which was developed for a flexible heat pipe under previous contract (Reference 1). The spiral multiwrap wick concept, Figure 3-1, consists of a spirally wrapped core of relatively coarse mesh screen which is encapsulated by a single layer of fine mesh screen. The coarse mesh interior is sized for self-priming in 1-g, and provides a high flow permeability, while the outer mesh provides a high capillary stress for good pumping. Since this type of wick is concentric with the container, it can easily be adapted to rotation simply by building in a planar gap at the rotating interface (Figure 3-2). The width of the gap, however, must be carefully controlled in order to assure that the wick will self-prime. Relative rotation of the rotating side of the wick with respect to the stationary side can be controlled through the use of a sleeve-type bearing as depicted in Figure 3-2. The gap in the sleeve bearing should be controlled to less than one-half the wire spacing in the

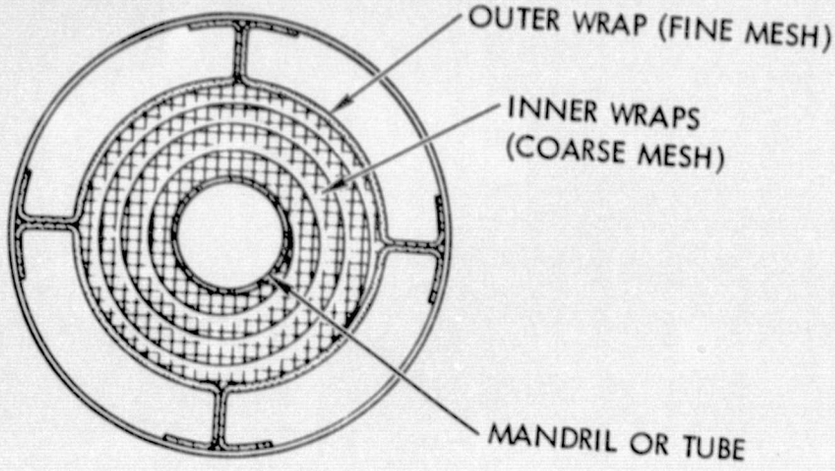

Figure 3-1. Spiral Multiwrap Wick Design

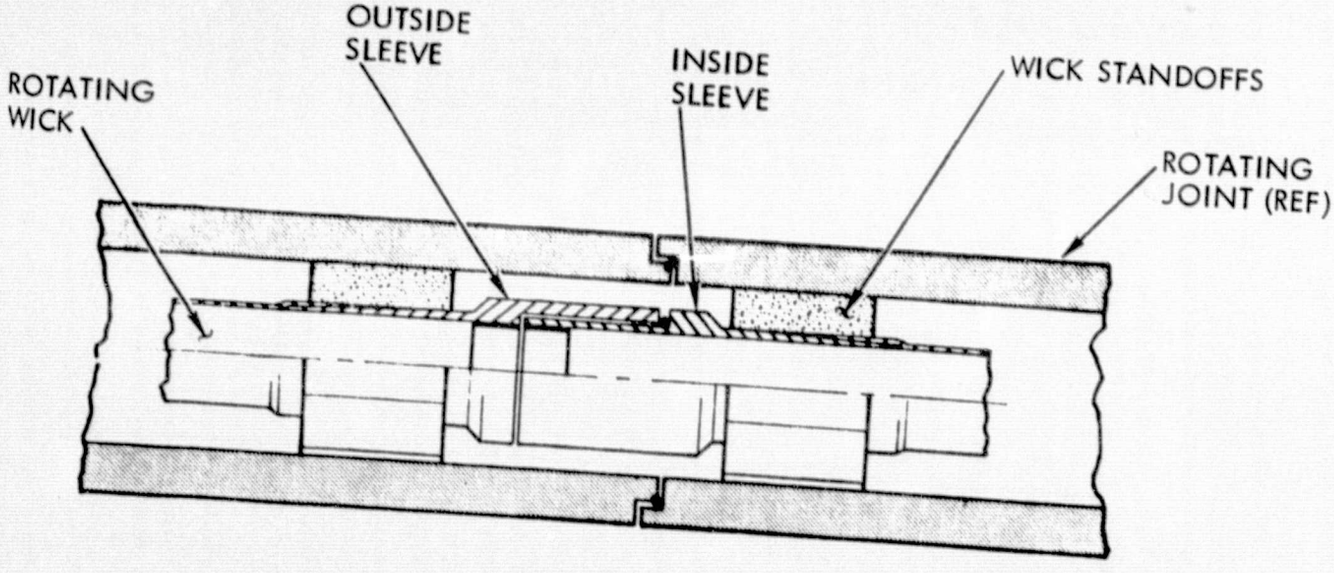

Figure 3-2. Rotating Wick Concept

fine mesh screen in order to provide at least the same level of capillary stress as the primary wick.

ROTATING WICK DESIGN AND FABRICATION

To demonstrate the rotating wick concept, a short (~12 cm long) wick was fabricated with a rotating interface in the center. The wick consists of two lengths of the basic spiral multiwrap wick assembly with a nylon sleeve bearing and support collar at the rotating interface. Figure 3-3 is a sketch of the longitudinal cross-section through the rotating wick assembly. As shown (Figure 3-3), the wick assembly is supported inside a plexiglass tube which also has a rotating O-ring seal to simulate the rotating heat pipe container.

Both the rotating and the stationary wick ends are fabricated by spirally wrapping 54-mesh screen onto a mandril. On the stationary side, the mandril is a 0.21-cm-diameter by 0.025-cm-wall 321 stainless-steel rod. This tube is slotted on the inside end and is used for filling and for bubble pressure testing the assembled wick joint. On the rotating end, the mandril is a 0.24 cm (0.093 in.) solid rod. The 54-mesh screen was selected because it would allow self-priming with most fluids, including methanol which was used for testing. The assembly was covered with an outer wrap of 200-mesh screen with an outside diameter of 0.64 cm (0.25 inch). After each section was cut to length (approximately 6 cm), an end cap was resistance-welded to each end. At the rotating interface, the end cap had four holes (see Figure 3-4) to allow fluid flow-through at the rotating interface. The disk-type end cap made it possible to control the gap to the precise tolerances required for self-priming (<0.025-cm gap width).

To align the wicks and maintain their position on the centerline of the container, nylon standoffs were machined to the configuration shown in Figure 3-5. The I.D.'s of both pieces were hand "honed" to fit snugly on each wick section. The wicks were set inside the nylon standoffs just enough so that the interface caps on the inside end of each wick just touched when the unit was assembled. Figure 3-6 shows the two wick pieces with the nylon bearing/standoffs attached. Figure 3-7 shows the assembled unit.

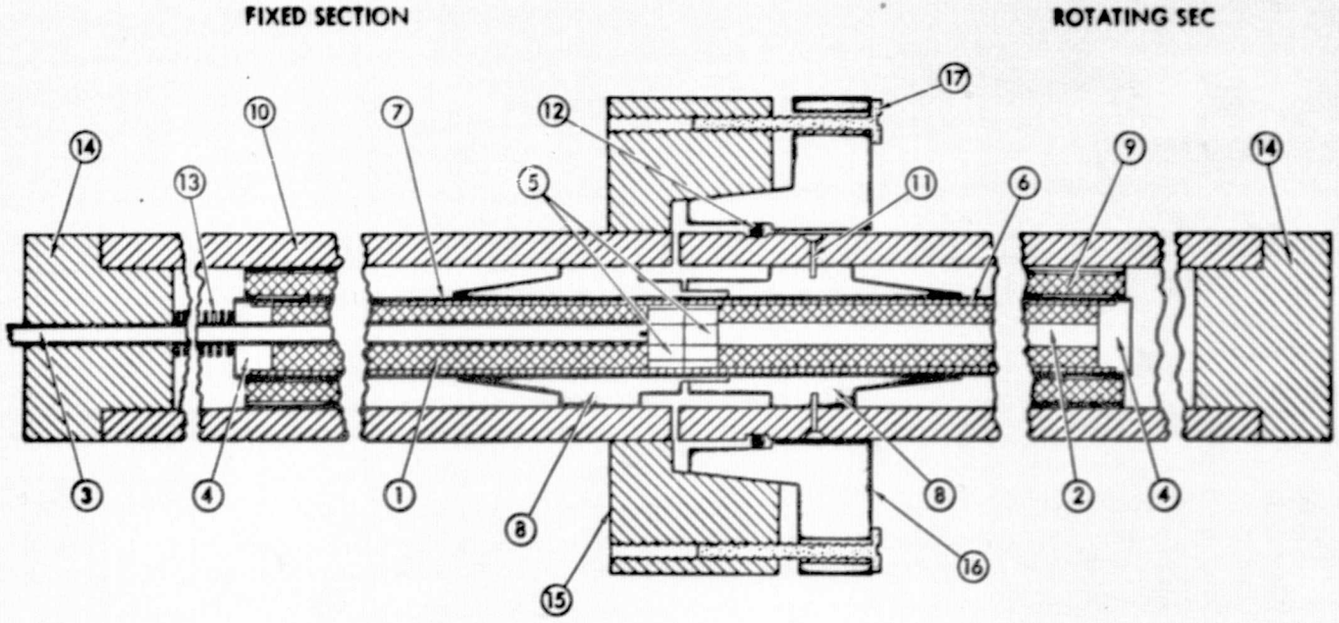

(1) - 54-MESH STAINLESS STEEL WICK
(2) - STAINLESS STEEL ROD
(3) - STAINLESS STEEL FILL TUBE
(4) - STAINLESS STEEL WICK END CAP
(5) - STAINLESS STEEL WICK INTERFACE CAP
(6) - 54-MESH STAINLESS STEEL LAYER
(7) - 200-MESH STAINLESS STEEL WICK OUTER LAYER
(8) - NYLON STANDOFF
(9) - 200-MESH STAINLESS STEEL SCREEN STANDOFF
(10) - ACRYLIC CONTAINER TUBE
(11) - STEEL PIN
(12) - O-RING
(13) - SPRING
(14) - ACRYLIC CONTAINER PLUG
(15) - ACRYLIC CONNECTOR
(16) - NYLON CONNECTOR
(17) - 6-32 SCREWS

Figure 3-3. Sketch of the Longitudinal Cross Section Through the Heat Pipe Wick Assembly

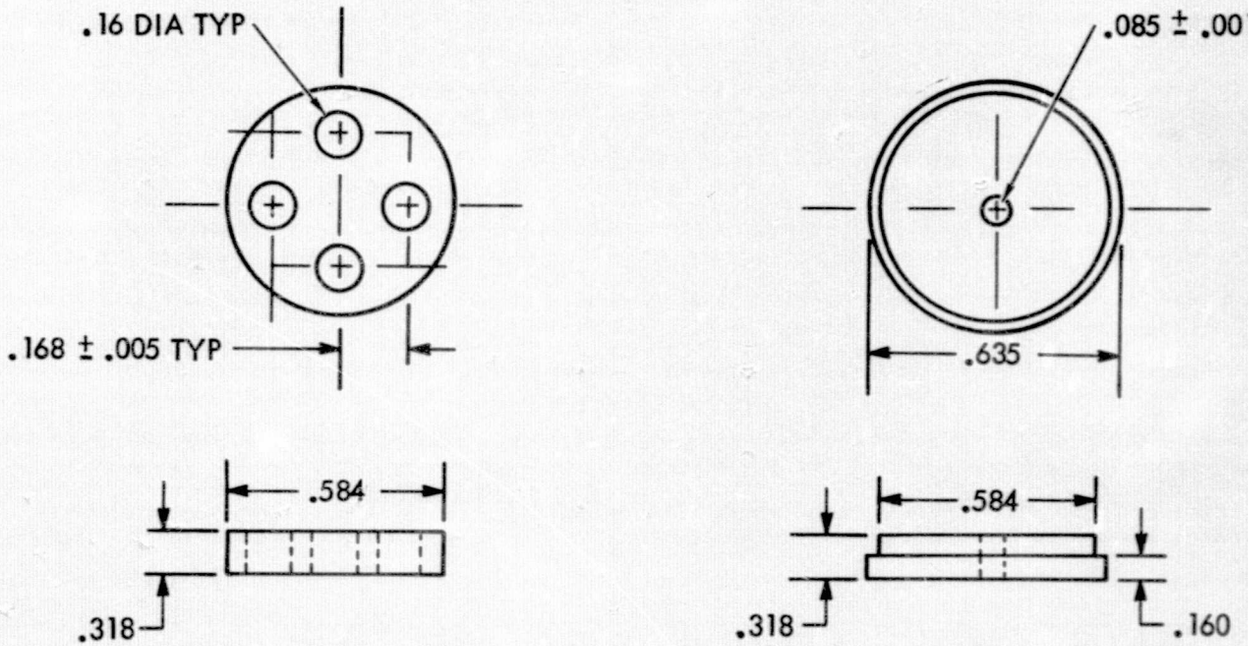

WICK INTERFACE CAP

NOT TO SCALE

DIM. ± .013 UNLESS OTHERWISE NOTED

*Dimensions in cm

WICK END CAP

MATERIAL - 321 STAINLESS STEEL

Figure 3-4. Wick Interface and End Caps

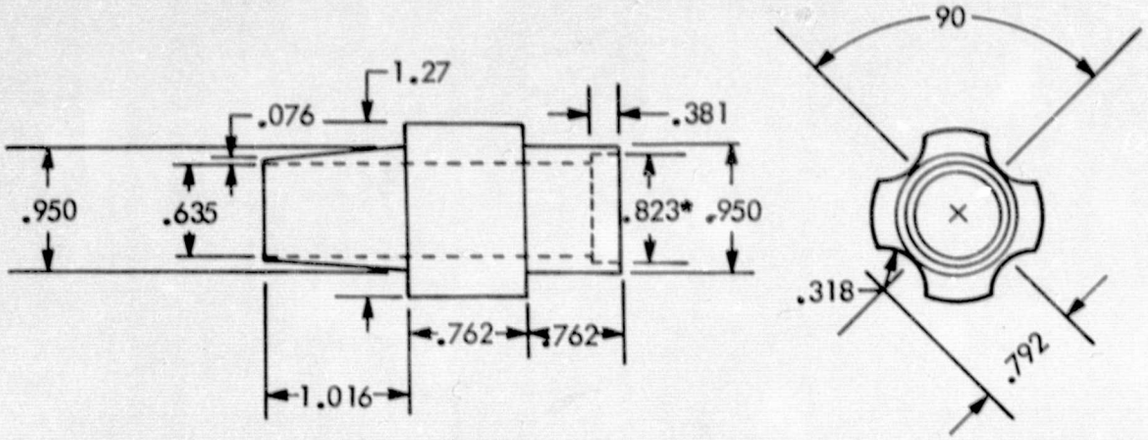

ROTATING SECTION

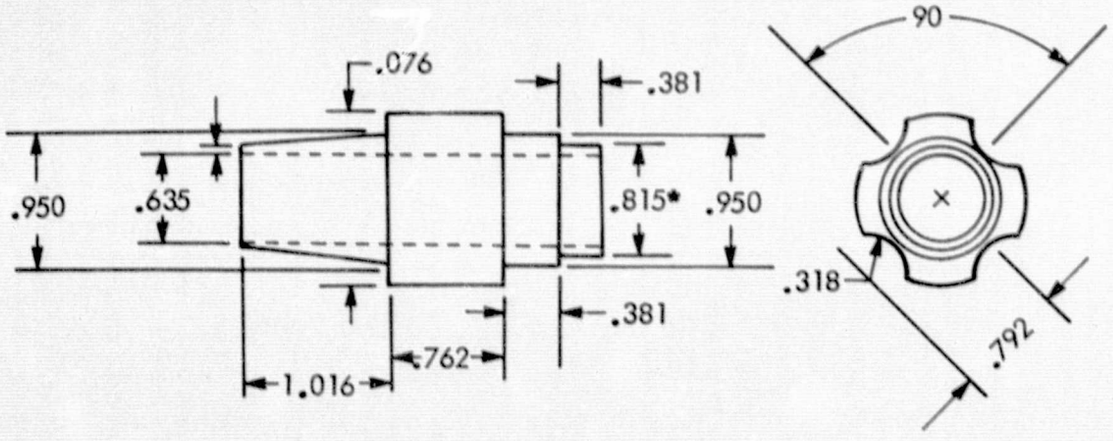

FIXED SECTION

NOT TO SCALE
DIM. ± .013 UNLESS OTHERWISE NOTED

*ACTUAL

Dimensions in cm

Figure 3-5. Nylon Standoffs

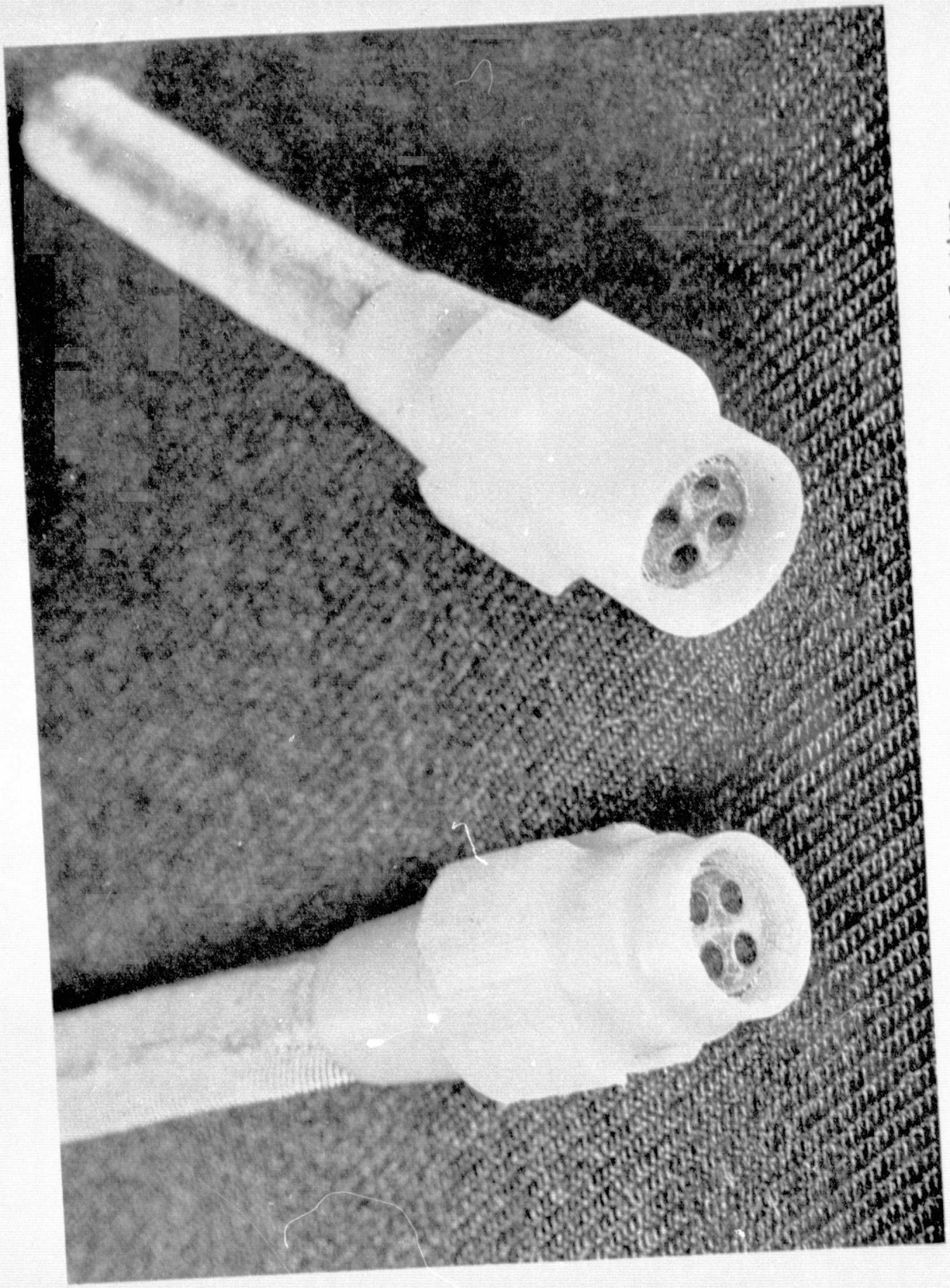

Figure 3-6. Nylon Standoffs Installed On Interface Ends of Wick Sections

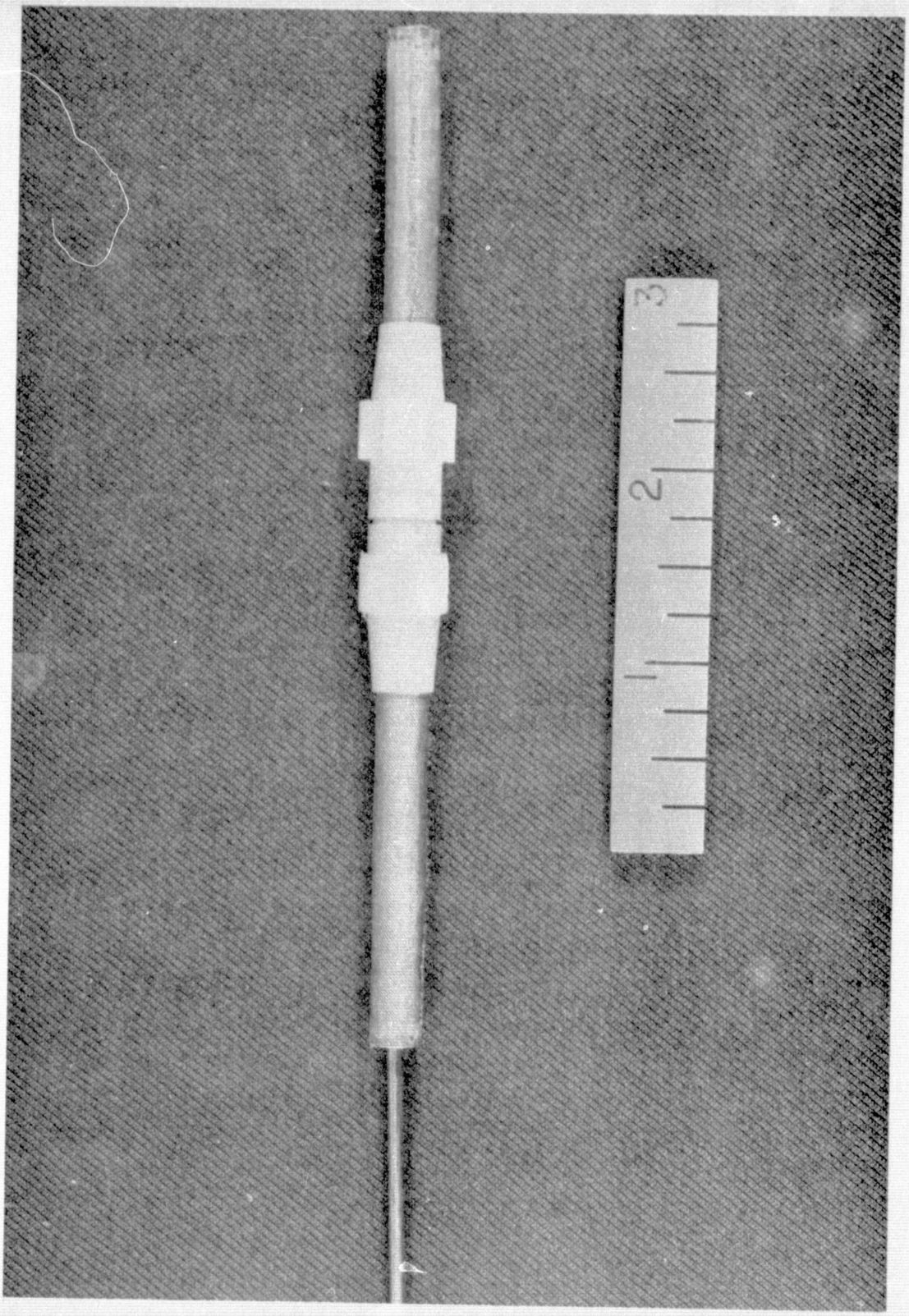

Figure 3-7. Subassembly of Wick Sections

WICK PERFORMANCE TESTS

To verify the performance of the assembled wick, two simple tests were performed—first, a bubble pressure test to determine the capillary pressure of the assembly, and finally, a self-priming test to verify that the wick would prime in a 1-g field. For the bubble pressure test, the wick assembly was submerged in a methanol bath such that the liquid just covered the entire wick. Nitrogen gas was pressurized into the wick through the fill tube, while the gas pressure was measured on a water nanometer. The test set-up is shown in Figure 3-8. The wick held a pressure of 6.6 to 6.7 cm of water under static and rotating conditions. For methanol at 293 K, the theoretical capillary pressure with 200-mesh screen is 6.86 cm of water, which agrees closely with the test data.

For the second test, the wick was allowed to dry thoroughly. A short piece of double-layer 200-mesh screen was attached to one end of the wick, and was inserted into a beaker of methanol while the wick was maintained horizontal on a platform balance (Figure 3-9). Figure 3-10 shows a close-up view of the self-priming test. Within approximately two minutes, the wick was thoroughly saturated, and had absorbed 2.6 g of methanol. The theoretical fill inventory for the wick assembly is 2.5 g, which agrees well with the test data.

FINAL ASSEMBLY

After the performance tests were completed, the wick was installed in a rotating plexiglass tube assembly to show how the wick would be held in place in a rotating heat pipe. The standoff wicks were fabricated from 200-mesh screen in accordance with the configuration shown in Figure 3-11. The standoff wicks would be used in a rotating heat pipe to transport the working fluid from the primary wick to the tube wall of the evaporator and condenser sections. These standoffs were resistance-welded onto either end of the rotating wick assembly. The entire wick assembly was inserted in a plexiglass tube which simulates the rotating heat pipe container. The plexiglass tube also has a rotating interface with an O-ring seal. The wick and tube components are shown in Figure 3-12. To keep the wick section positioned longitudinally—as well as to prevent rotation slippage—two 0.053-cm-diameter holes were match-drilled, 180 degrees apart, through the acrylic tube and into the

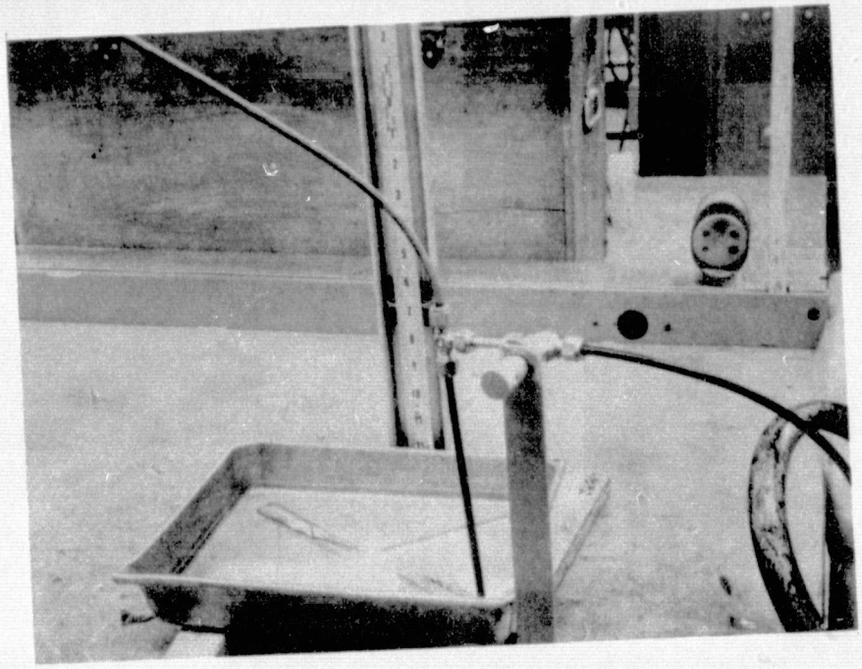

Figure 3-8. Static Pressure Test

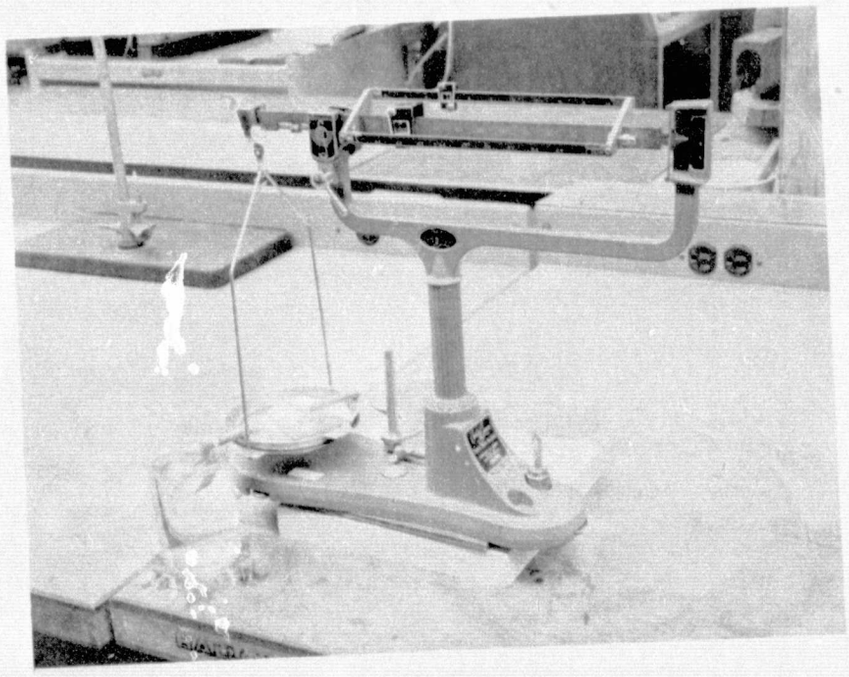

Figure 3-9. Overall View of Wick Saturation Test

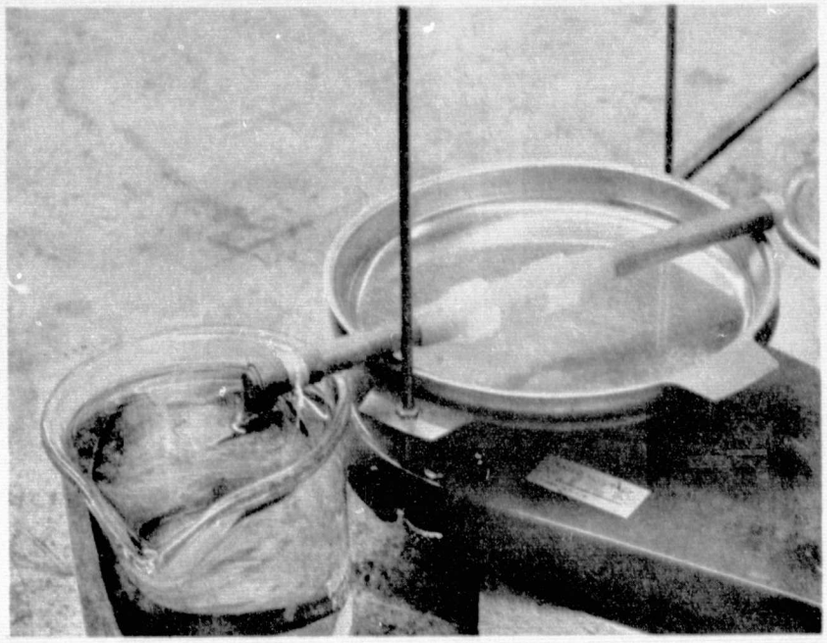

Figure 3-10. Close-Up View of Wick Saturation Test

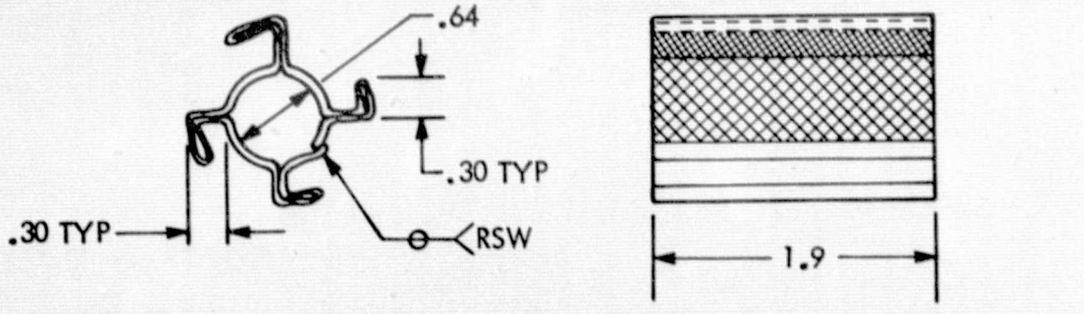

Figure 3-11. Screen Standoff Configuration

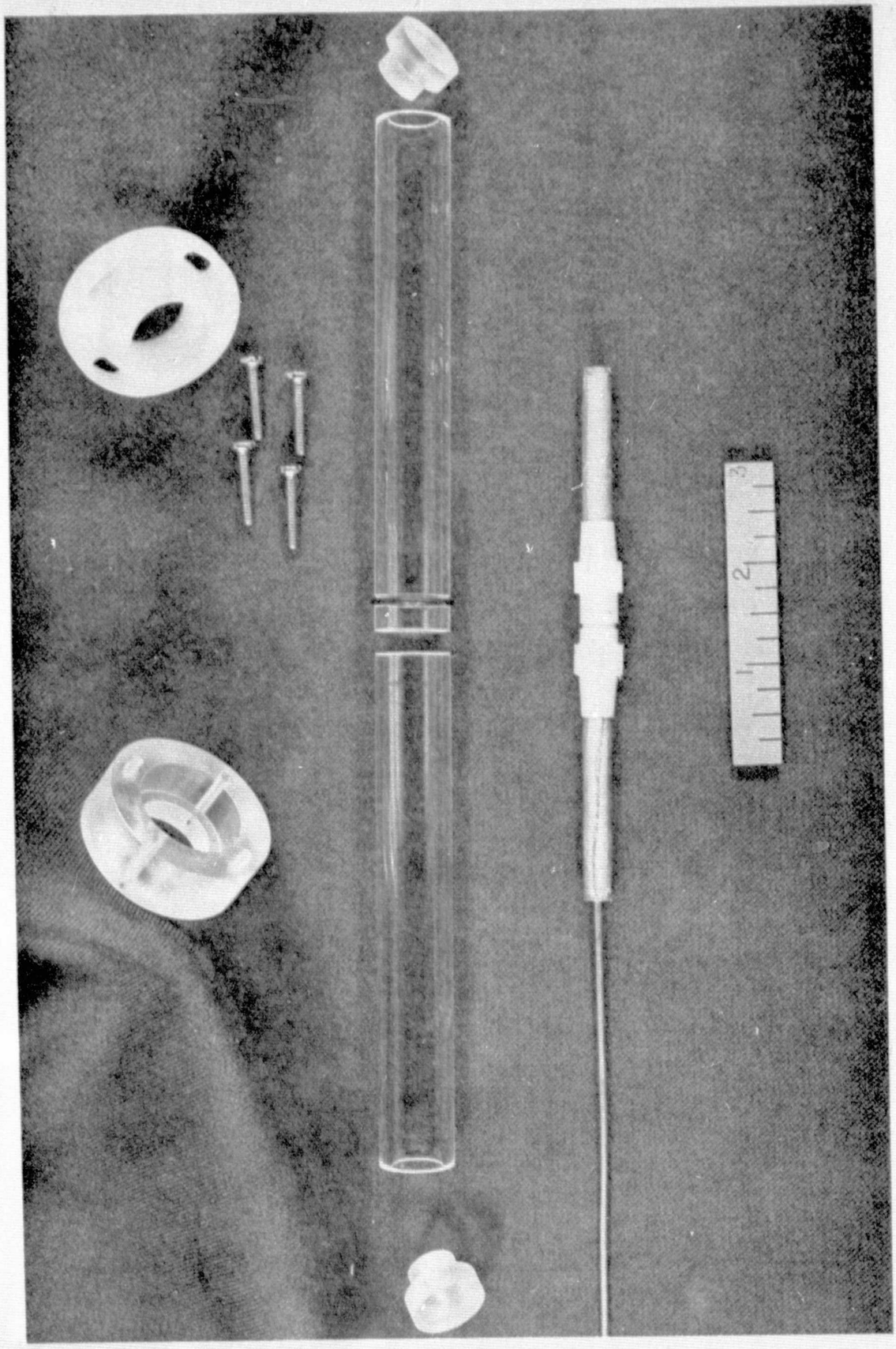

Figure 3-12. Photograph of the Heat Pipe Wick Assembly Details

nylon standoffs. The holes were countersunk and two steel pins, cut to 0.953 cm, were inserted so that the pinheads were flush with the O.D. surface. Figure 3-13 is a close-up photograph of this installation that also shows the O-ring in the machined groove.

To insure contact between the interface caps, a spring was put around the fill tube so that a slight pressure was exerted on the back of the rotating wick section when the container plug was installed. Figure 3-14 shows the assembled wick and plexiglass container.

Figure 3-13. Wick Section Installation In the Rotating Side of the Container

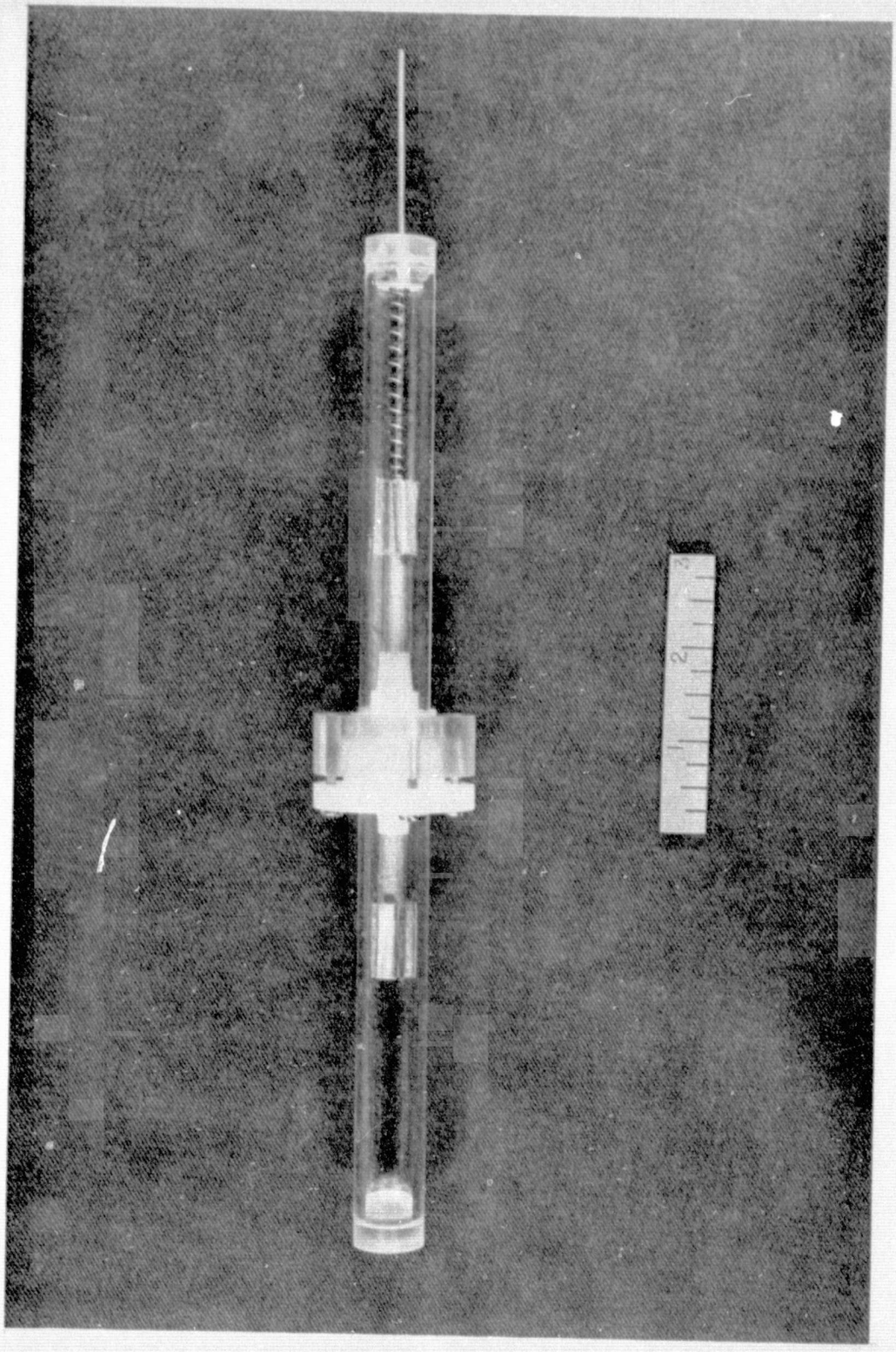

Figure 3-14. Photograph of the Completed Heat Pipe Wick Assembly

4.0 CONCLUSIONS AND RECOMMENDATIONS

In attempting to develop rotatable cotainer and wick components for a rotating heat pipe, the container proved to be by far the more difficult task. At the outset of the program, it was known that the design goal leakage rate of 10^{-6} atm-cc/sec (sccs) would be difficult to achieve. The primary factors which render the leakage containment problem so difficult are the combined requirements for cryogenic temperature operation and high internal pressure containment. The selected design approach, which involves the use of a spring-loaded ring seal and highly polished sealing surfaces, was felt to be the most practical in terms of meeting the pressure and temperature requirements. A similar concept was used on a rotating pump seal for the Space Shuttle main engine (SSME) fuel lines. The selected seal material, amorphous Kel-F, was felt to have the best compromise of physical and mechanical properties. As it turned out, the amorphous Kel-F material was extremely sensitive to frictional wear, and was damaged after less than 42 revolutions at ambient temperature. Static helium leakage rates were initially high (1.4×10^{-3} sccs), but reduced to $<2\times10^{-5}$ sccs at 293 K and 0.4 MPa after 25 wear-in cycles. This is still over an order of magnitude above the design goal leak rate. Under dynamic conditions (4 rev/hr rotation), the leakage rates were higher compared to the static test values. At 293 K and 4 rev/hr rotation, the dynamic leakage varied between 10^{-4} and 3×10^{-4} sccs, well above the design goal. The rotational torque was approximately .6 N-m at 293 K, although the initial breakaway torque was almost twice as high.

Testing of the Kel-F seal was discontinued when it was discovered that the seal was damaged after only 42 wear-in cycles. Inspection revealed that flakes of the seal material had worn off during the wear-in, and adhered to the metallic sealing surfaces. Discussions were held with the seal manufacturer, and it was concluded that the amorphous Kel-F material, while having good properties at cryogenic temperature, was not conducive to a long-wear life at ambient temperature. The manufacturer felt that possibly some intermediate between amorphous and crystalline Kel-F would withstand the frictional

wear-in forces and still have good sealing qualities at cryogenic temperatures. Because of the limited scope of the program, however, other seals were not evaluated under this contract. No cryogenic test data were obtained since both the primary and the spare Kel-F seals were damaged during wear-in.

Independent tests were conducted at Rockwell using a seal made from TFE Teflon with 12-15% carbon graphite added. Initial static leakage levels were comparable to Kel-F, and reduced to 5×10^{-5} sccs at 0.4 MPa after 400 wear-in cycles. This leakage rate is somewhat lower than the calculated permeability limit of the Teflon material at 293 K. When the shaft was rotated at 4 rev/hr, a leakage rate of 6×10^{-5} sccs was observed. At cryogenic temperature, both the static and dynamic leakage rates increased substantially to 2.6×10^{-2} sccs and 1.6×10^{-2} sccs, respectively. In the way of explanation, it was hypothesized that the seal may have distorted during thermal contraction. The increased surface hardness of the material at cryogenic temperature may also explain to some degree the increase in leak rate. Also, a change in the Teflon from an amorphous structure to a crystalline structure at cryogenic temperature may be partially responsible. Additional testing and development is needed to discern the causes of the increase in leak rate and, hopefully, to find a combination of seal material and configuration which will meet the design goal leakage rate of 10^{-6} sccs.

Rotational torque on the Teflon/graphite seal was very low compared to the Kel-F and to the 3-5 N-m design requirement. At 293 K, the rotational torque was 0.1 N-m. At 100 K, the torque was less than 0.6 N-m (some of this torque was due to the rotary feedthrough to the vacuum chamber).

The rotatable wick joint functioned successfully in both the bubble pressure and self-priming tests. The most critical element of the design was the gap between the two sides of the wick at the rotational interface. The required gap width for the 0.64-cm-diameter wick tested was ~0.025 cm. A porous end plug was attached to the opposing surfaces of the two wick sections to guarantee a smooth, flat surface. The spiral multiwrap wick design proved to be very conducive to adding the rotating interface, although other cylindrical composite or homogeneous wick designs could also be used.

In conclusion, the feasibility of a cryogenic rotatable heat pipe for long-term space operation hinges on reducing the leakage to an acceptable level. For some heat pipe working fluids, the achieved dynamic leakage rate of 2×10^{-4} sccs may be acceptable for operation up to one year. Additional testing and development with Teflon/graphite and other seal materials is recommended. After acceptable leakage levels have been attained, fabrication and testing of a rotatable heat pipe is also recommended.

REFERENCES

1. "Flexible Cryogenic Heat Pipe Development Program - Final Report" NASA CR 152027, Contract NAS2-8830, Rockwell Report No. SD77-AP-0088, July 1977.

2. Internal Memo IL9137-2015, "Final Report - J-28 LOX Valve Shaft Seal Development", May 5, 1969, Rocketdyne Division, Rockwell International Corp.

3. "Heat Pipe Technology - CFY 1978 Final IR&D Report", Rockwell International Corp., (To be Published).

PAGE 64 INTENTIONALLY BLANK